ARTICLE

Check for updates

Adipocyte G_q signaling is a regulator of glucose and lipid homeostasis in mice

Takefumi Kimura[1,7], Sai P. Pydi[1], Lei Wang[1], Dhanush Haspula[1], Yinghong Cui[1], Huiyan Lu[2], Gabriele M. König[3], Evi Kostenis [4], Gregory R. Steinberg [5], Oksana Gavrilova[6] & Jürgen Wess [1✉]

Obesity is the major driver of the global epidemic in type 2 diabetes (T2D). In individuals with obesity, impaired insulin action leads to increased lipolysis in adipocytes, resulting in elevated plasma free fatty acid (FFA) levels that promote peripheral insulin resistance, a hallmark of T2D. Here we show, by using a combined genetic/biochemical/pharmacologic approach, that increased adipocyte lipolysis can be prevented by selective activation of adipocyte G_q signaling in vitro and in vivo (in mice). Activation of this pathway by a G_q-coupled designer receptor or by an agonist acting on an endogenous adipocyte G_q-coupled receptor (CysLT$_2$ receptor) greatly improved glucose and lipid homeostasis in obese mice or in mice with adipocyte insulin receptor deficiency. Our findings identify adipocyte G_q signaling as an essential regulator of whole-body glucose and lipid homeostasis and should inform the development of novel classes of GPCR-based antidiabetic drugs.

[1] Molecular Signaling Section, Laboratory of Bioorganic Chemistry, National Institute of Diabetes and Digestive and Kidney Diseases, Bethesda, MD 20892, USA. [2] Mouse Transgenic Core Facility, National Institute of Diabetes and Digestive and Kidney Diseases, Bethesda, MD 20892, USA. [3] Institute of Pharmaceutical Biology, University of Bonn, 53115 Bonn, Germany. [4] Molecular, Cellular and Pharmacobiology Section, Institute of Pharmaceutical Biology, University of Bonn, 53115 Bonn, Germany. [5] Center for Metabolism, Obesity and Diabetes Research, Department of Medicine and Department of Biochemistry and Biomedical Sciences, McMaster University, Hamilton, ON L8K 4P1, Canada. [6] Mouse Metabolism Core National Institute of Diabetes and Digestive and Kidney Diseases, Bethesda, MD 20892, USA. [7] Present address: Department of Medicine, Division of Gastroenterology and hepatology, Shinshu University School of Medicine, Matsumoto 390-8621, Japan. ✉email: jurgenw@niddk.nih.gov

Adipocytes play an important role in the pathogenesis of type 2 diabetes (T2D), and white adipose tissue (WAT) contributes to the regulation of whole-body glucose and energy homeostasis[1–3]. Obesity is characterized by an excess of WAT, associated with an increase in adipocyte size due to increased triglyceride (TG) deposition[4]. Lipolysis in white adipocytes is increased in the obese state, resulting in the release of excessive amounts of free fatty acids (FFAs) into the blood stream[2,4]. This increase in lipolysis is thought to be caused by a decrease in the responsiveness of WAT to the antilipolytic action of insulin[4]. Increased plasma FFA levels lead to the ectopic accumulation of fat in other peripheral tissues involved in the regulation of glucose homeostasis, contributing to peripheral insulin resistance and impaired glucose tolerance[1–3]. In combination with compromised β-cell function, impaired peripheral insulin action eventually leads to the development of T2D[5]. On the basis of these considerations, adipocytes are considered excellent drug targets to improve impaired glucose homeostasis in T2D and related metabolic disorders[2].

G protein-coupled receptors (GPCRs) are known to regulate key metabolic processes including whole-body glucose and energy homeostasis[6–8]. GPCRs represent a superfamily of cell surface receptors that respond to a large variety of extracellular signals including hormones, neurotransmitters, paracrine factors, and many other agents and stimuli[9,10]. About 30–40% of drugs in current clinical use act on one or more distinct GPCRs, indicative of the extraordinary clinical relevance of this class of receptors[9].

Like all other cell types, adipocytes express dozens of GPCRs which are coupled to different functional classes of heterotrimeric G proteins[11,12]. Based on the structural and functional properties of the G protein α subunits, heterotrimeric G proteins are subdivided into four major classes: G_s, $G_{i/o}$, $G_{q/11}$, and $G_{12/13}$[13]. Previous studies have shown that stimulation of adipocyte G_s signaling promotes lipolysis, while activation of adipocyte G_i signaling exerts antilipolytic effects[11,14–17]. In contrast, little is known about the in vivo metabolic consequences of selectively activating G_q signaling in adipocytes.

To address this issue, we used a chemogenetic approach to generate a mouse model that expresses a G_q-coupled designer GPCR (G_q DREADD; G_q-Coupled Designer Receptor Exclusively Activated by a Designer Drug; alternative names: hM3Dq or simply GqD)[18,19] selectively in adipocytes (adipo-GqD mice). Treatment of adipo-GqD mice with clozapine-N-oxide (CNO), a synthetic compound that can activate GqD and related DREADDs but is otherwise pharmacologically inert when used in the proper dose/concentration range[18,19], selectively stimulated G_q signaling in adipocytes. We also generated and analyzed several additional mutant mouse models to explore the cellular and molecular mechanisms underlying the metabolic changes caused by the activation of adipocyte G_q signaling.

Here, we show that activation of adipocyte G_q signaling improves glucose homeostasis and peripheral insulin sensitivity under both physiological and pathophysiological conditions. In vitro and in vivo studies demonstrated that agents that activate adipocyte G_q signaling inhibit lipolysis and stimulate glucose uptake in an insulin-independent fashion in both human and mouse adipocytes, leading to reduced plasma FFA levels and improved glucose tolerance. We also demonstrated that activation of a G_q-coupled receptor (CysLT$_2$ receptor) that is endogenously expressed by both mouse and human adipocytes mimics the beneficial metabolic effects observed with CNO-treated adipo-GqD mice. Our findings indicate that adipocyte G_q signaling represents a key regulator of whole-body lipid and glucose homeostasis. The identification of drugs able to selectively activate G_q-coupled receptors endogenously expressed by adipocytes may lead to novel therapies for the management of T2D.

Results

Selective activation of adipocyte G_q signaling in vivo improves glucose homeostasis. To be able to selectively activate G_q signaling in adipocytes in vivo, we used a CNO-sensitive designer GPCR that selectivity couples to G proteins of the G_q family as a tool (official name: hM3Dq; alternative names: G_q DREADD or simply GqD)[18,19]. To generate mutant mice that express the GqD receptor selectively in adipocytes (adipo-GqD mice), we crossed *LSL-hM3Dq* mice[20] with *adipoq-Cre* mice[21]. Adipo-GqD mice carried one copy of the *LSL-GqD* allele and one copy of the *adipoq-Cre* transgene. *LSL-hM3Dq* mice that did not harbor the *adipoq-Cre* transgene served as control animals throughout all experiments. qRT-PCR studies confirmed that GqD was selectively expressed in adipose tissues of adipo-GqD mice (Fig. 1a).

Initially, we carried out metabolic studies with adipo-GqD mice and their control littermates (males that were at least 8 weeks old) maintained on regular chow diet. Bodyweight did not differ significantly between the two groups of mice (Fig. 1b). Acute CNO treatment (10 mg/kg i.p) led to a pronounced reduction in blood glucose levels in adipo-GqD mice, but not in control littermates (Fig. 1c). In both groups of mice, CNO administration had no significant effect on blood glucose excursions in glucose and insulin tolerance tests (glucose dose: 2 g/kg i.p.; insulin dose: 0.75 U/kg i.p.) (Fig. 1d, e). While CNO treatment did not affect plasma leptin levels in both cohorts of mice (Fig. 1f), CNO caused a significant reduction in plasma FFA levels in adipo-GqD mice (Fig. 1g), indicating that activation of adipocyte G_q signaling inhibits lipolysis. Basal plasma insulin levels after a 4 hr fast did not differ significantly between control and adipo-GqD mice (0.58 ± 0.07 ng/ml and 0.44 ± 0.06 ng/ml, respectively) (means ± s.e.m., $n = 10$ per group). CNO treatment (10 mg/kg i.p) of adipo-GqD mice had no significant effect on plasma insulin levels (0.42 ± 0.07 ng/ml; 30 min post-injection).

Treatment of adipo-GqD mice with a lower dose of CNO (3 mg/kg i.p.) or a very low dose (10 μg/kg i.p.) of another DREADD agonist, deschloroclozapine (DCZ)[22], led to comparable decreases in blood glucose and plasma FFA levels (Supplementary Fig. 1). This observation indicated that the metabolic phenotypes observed after treatment of mice with 10 mg/kg of CNO were not caused by any unspecific effects under our experimental conditions. CNO-injected control mice showed a trend towards increased plasma FFA levels, most likely as a consequence of the injection stress (Supplementary Fig. 1b). In agreement with this notion, injection of control and adipo-GqD mice with saline caused comparable increases in plasma FFA levels (Supplementary Fig. 1c). However, these responses failed to reach statistical significance.

We next carried out a similar series of experiments using adipo-GqD mice and control littermates (males) maintained on a high-fat diet (HFD) for at least 8 weeks. In male C57BL/6 mice, the genetic background on which the adipo-GqD mice were maintained, this obesogenic diet causes glucose intolerance, hyperglycemia, and insulin resistance, which are all key features of T2D[23,24]. Bodyweight and body composition (lean and fat body mass) did not differ significantly between HFD adipo-GqD and control mice maintained on HFD for 10 weeks (Fig. 2a, b). While acute CNO treatment (10 mg/kg i.p.) of HFD control mice had little effect on blood glucose levels, CNO-treated HFD adipo-GqD mice displayed a striking reduction in blood glucose levels (Fig. 2c).

In the absence of co-injected CNO, HFD adipo-GqD and control mice showed comparable impairments in glucose tolerance and insulin sensitivity (Fig. 2d, f). In contrast, following co-injection of glucose (1 g/kg i.p.) or insulin (1 U/kg i.p.) with CNO (10 mg/kg i.p.), HFD adipo-GqD mice displayed significant improvements in glucose tolerance and insulin sensitivity, respectively (Fig. 2e, g). Following co-injection of glucose
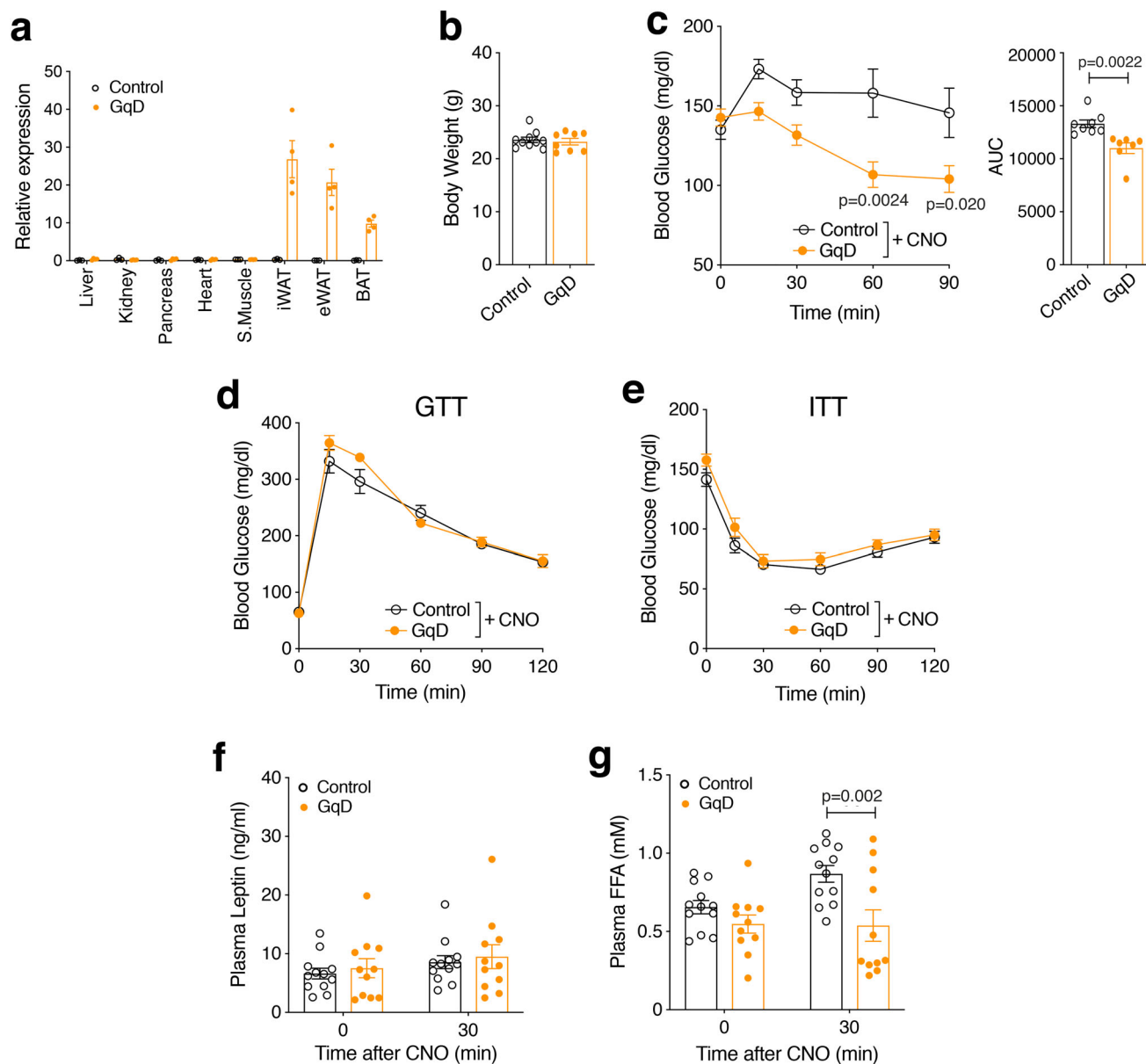
Fig. 1 Acute CNO treatment of adipo-GqD mice causes reduced blood glucose and plasma free acid levels. a Expression levels of GqD mRNA in different tissues of adipo-GqD (GqD) and control mice (*LSL-hM3Dq* mice that did not harbor the *adipoq-Cre* transgene) ($n = 4$ per group). The presence of GqD transcripts was detected via qRT-PCR. S. Muscle, skeletal muscle; iWAT, inguinal white adipose tissue; eWAT, epididymal white adipose tissue; BAT, brown adipose tissue. **b** Body weights of adipo-GqD and control mice (mouse age: 12 weeks; $n = 8$–10 per group). **c** Blood glucose levels after CNO injection (10 mg/kg i.p.) following a 4 hr fast ($n = 7$–9 per group). **d**, **e** Effect of acute CNO treatment (10 mg/kg i.p.) on glucose tolerance (**d**, GTT) and insulin tolerance (**e**, ITT). GTT: 2 g glucose/kg after an overnight fast; ITT: 0.75 U insulin/kg after a 4 hr fast ($n = 8$ or 9 per group). **f**, **g**, Plasma leptin (**f**), and plasma free fatty acid (FFA) (**g**) levels of control and adipo-GqD mice 30 min after injection of CNO (10 mg/kg i.p.) following a 4 hr fast ($n = 11$ or 12 per group). Metabolic tests (**c**–**g**) were carried out with male mice that were 10-16 weeks old. Data are presented as means ± s.e.m. **b**, **c** (AUC), **f**, **g**: two tailed Student's *t*-test; **c**–**e**: two-way ANOVA followed by Bonferroni's post hoc test). Source data are provided as a Source data file.

(1 g/kg i.p.) with CNO, glucose-stimulated insulin secretion (GSIS) was significantly reduced in HFD adipo-GqD mice, as compared to the corresponding control animals (Fig. 2h), most likely as a result of improved glucose homeostasis caused by adipocyte G_q activation. In agreement with the plasma FFA data obtained with mice maintained on regular chow (Fig. 1g), CNO treatment caused a significant reduction in plasma FFA and glycerol levels in HFD adipo-GqD mice (Fig. 2i, j). This CNO effect was not observed with HFD control littermates (Fig. 2i, j), confirming that activation of adipocyte G_q signaling inhibits lipolysis in vivo. CNO treatment had no significant effect on plasma leptin levels in both groups of mice (Fig. 2k).

To explore the metabolic effects of chronic activation of adipocyte G_q signaling, we injected adipo-GqD mice and control littermates consuming regular chow daily with CNO (10 mg/kg i.p.) for 11 days (Supplementary Fig. 2). While chronic CNO treatment did not lead to any genotype-dependent changes in body weight and insulin tolerance (Supplementary Fig. 2a, c), CNO-treated adipo-GqD mice showed improved glucose tolerance (Supplementary Fig. 2b). Moreover, following repeated CNO treatment, adipo-GqD mice consistently displayed significantly reduced plasma FFA levels (Supplementary Fig. 2d). In contrast, chronic CNO treatment of control littermates had no significant effect on plasma FFA levels (Supplementary Fig. 2d). These data
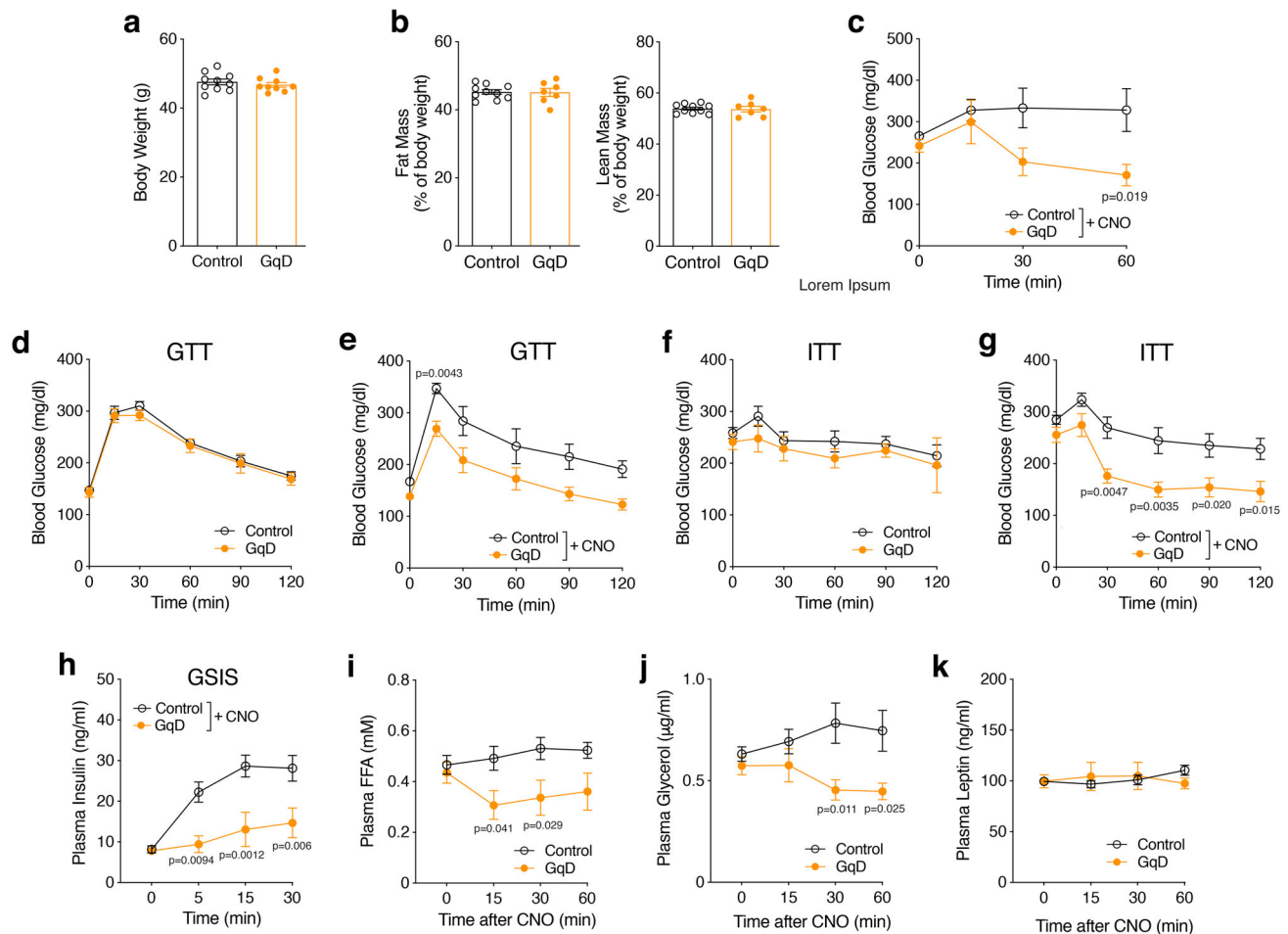
Fig. 2 Acute CNO treatment of adipo-GqD mice maintained on an obesogenic diet improves glucose homeostasis and suppresses lipolysis. a, b Body weight (**a**) and body composition (fat and lean mass as % of body weight) (**b**) of adipo-GqD and control mice maintained on high-fat diet (HFD) for 10 weeks prior to CNO treatment ($n = 7$–10 per group). *LSL-hM3Dq* mice that did not harbor the *adipoq-Cre* transgene served as control animals throughout all experiments. **c** Blood glucose levels of HFD adipo-GqD and control mice after acute treatment with CNO (10 mg/kg i.p.) following a 4 hr fast. **d, e** Glucose tolerance test (GTT) without (**d**) and with (**e**) CNO treatment (10 mg/kg i.p.) after an overnight fast (16 hr). **f, g** Insulin tolerance test (ITT) without (**f**) and with (**g**) CNO treatment (10 mg/kg i.p.) after a 4 h fast. **h** Glucose-stimulated insulin secretion (GSIS). Plasma insulin levels of HFD adipo-GqD and control mice after i. p. treatment with glucose (2 g/kg) plus CNO (10 mg/kg) after a 4 h fast. **i–k** Plasma FFA (**i**), glycerol (**j**) and leptin (**k**) levels of HFD control and adipo-GqD mice after acute treatment with CNO (10 mg/kg i.p.) following a 4 h fast. In (**c–k**) mice were maintained on HFD for 10–14 weeks ($n = 5$–10 per group). Data are shown as means ± s.e.m. **c–k**: two-way ANOVA followed by Bonferroni's post hoc test). Source data are provided as a Source data file.

indicate that chronic activation of adipocyte G_q signaling also results in significant metabolic improvements in mice.

CNO treatment of adipo-GqD mice promotes glucose uptake by inguinal WAT and heart. To examine whether activation of adipocyte G_q signaling promoted glucose uptake into adipose tissues, we performed an in vivo ^{14}C-2-deoxyglucose (^{14}C-2-DG) uptake assay (Supplementary Fig. 3a). Adipo-GqD mice and control littermates were fasted overnight and then injected with CNO (10 mg/kg i.p.) and a trace amount of ^{14}C-2-DG. Forty min later, the mice were euthanized, and the ^{14}C-2-DG content of inguinal WAT (iWAT), epididymal WAT (eWAT), brown adipose tissue (BAT), various skeletal muscle tissues, heart, and liver was determined. We found that CNO treatment caused a significant increase in stimulated glucose uptake (^{14}C-2-DG accumulation) in iWAT and heart of adipo-GqD mice (Supplementary Fig. 3a).

One possible explanation for the increase in cardiac glucose uptake displayed by the adipo-GqD mice is that the CNO-

induced lowering of plasma FFA levels resulting from activation of adipocyte G_q signaling led to an increased usage of glucose as a cardiac fuel source[25,26]. To further corroborate this concept, we subjected mice that expressed a G_i-coupled DREADD selectively in adipocytes (adipo-GiD mice)[14] to ^{14}C-2-DG uptake studies. We previously demonstrated that CNO treatment of adipo-GiD mice results in greatly reduced plasma FFA acid levels[14], similar to our current findings with CNO-treated adipo-GqD mice. In agreement with the data obtained with the adipo-GqD mice (Supplementary Fig. 3a), CNO (10 mg/kg i.p.) treatment of adipo-GiD mice resulted in a significant increase in ^{14}C-2-DG uptake in the heart (Supplementary Fig. 3b). Taken together, these data are in agreement with previous studies that lowering of plasma FFA levels promotes the usage of glucose as a cardiac fuel source.

Functional and biochemical studies with differentiated mouse 3T3F442A adipocytes. To gain insight into the cellular and molecular mechanisms through which activation of adipocyte G_q signaling exerts its beneficial metabolic actions in vivo, we carried

out studies with cultured, fully differentiated 3T3F442A mouse adipocytes. Infection of 3T3F442A cells with an adenovirus coding for GqD resulted in GqD-expressing 3T3F442A cells (GqD-3T3F442A cells) (Supplementary Fig. 4a). For control purposes, we infected 3T3F442A cells with an adenovirus encoding GFP, resulting in GFP-3T3F442A control cells. In experiments exploring the functional properties of GqD- and GFP-3T3F442A cells, both cell lines were processed in parallel.

Western blotting studies demonstrated that CNO (10 µM) treatment of differentiated GqD-3T3F442A cells promoted the phosphorylation of AMPK and AS160 (Tbc1d4) (Fig. 3a, b) (see Supplementary Fig. 5a for the specificity of the AS160 antibody). These effects could be blocked by co-incubation with FR900359 (FR; 1 µM), a selective inhibitor of $G_{q/11}$[27] (Fig. 3c, d). Cell fractionation studies showed that incubation of GqD-3T3F442A cells with CNO (10 µM) resulted in a pronounced translocation of GLUT4 to the plasma membrane (Fig. 3e, f), a response that is typically observed after activation of AMPK signaling in adipocytes[28]. The magnitude of this response was similar to that of 10 nM insulin. At the same time, CNO treatment of GqD-3T3F442A cells resulted in reduced levels of cytoplasmic GLUT4 (Supplementary Fig. 5b). CNO (10 µM) treatment of GFP-3T3F442A control cells had no significant effect on the phosphorylation status of AMPK or GLUT4 translocation (Supplementary Fig. 4b, c).

Hormone-sensitive lipase (HSL) catalyzes a key step in the breakdown of triglycerides[29]. Previous studies have shown that activated AMPK phosphorylates HSL at S565, resulting in the inhibition of HSL activity[30,31]. In agreement with the observed increase in pAMPK levels (Fig. 3a, b), CNO treatment of GqD-3T3F442A cells stimulated the phosphorylation of HSL at S565 (Fig. 3e, f). In contrast, treatment of GqD-3T3F442A cells with CL316,243 (100 nM), a β3-adrenergic receptor (β3-AR) agonist that leads to G_s-dependent activation of PKA, had no significant effect on the phosphorylation status of S565 (Fig. 3g, h). However, co-incubation of GqD-3T3F442A cells with CL316,243 and CNO promoted HSL phosphorylation at S565, as compared to treatment with CL316,243 alone (Fig. 3g, h).

To explore whether similar changes occurred in vivo, we injected adipo-GqD mice and control littermates with CNO (10 mg/kg i.p.) and then harvested iWAT 5 min later. Western blotting studies confirmed that CNO-stimulated adipocyte G_q signaling promoted the accumulation of pAMPK and pHSL(S565) in iWAT (Supplementary Fig. 6). These data agree very well with the in vitro data described in the previous paragraph.

We next examined whether CNO treatment was able to promote glucose uptake in differentiated GqD-3T3F442A cells, using the ^{14}C-2-deoxy-D-glucose (2-DG) method. While CNO (10 µM) had no significant effect on glucose uptake in GFP-3T3F442A control cells, it caused a ~twofold increase in glucose uptake in GqD-3T3F442A cells (Fig. 4a). The stimulatory effect of GqD activation on glucose uptake was abolished by incubation of GqD-3T3F442A cells with FR900359 ($G_{q/11}$ inhibitor; 1 µM), BAPTA (Ca^{2+} chelator, 10 µM), and Compound C (AMPK inhibitor, 10 µM) (Fig. 4b-d). We also noted that CNO treatment of GqD-3T3F442A cells stimulated the activity of CaM kinase (CaMK) kinase 2 (CAMKK2) by ~4-fold (Fig. 4e). This stimulatory CNO effect could be greatly reduced by incubation of GqD-3T3F442A cells with STO-609 (2 µM), a selective inhibitor of CAMKK2 (Fig. 4e). These observations support a model in which G_q-induced glucose uptake by adipocytes depends on the known ability of activated $G_{q/11}$ to increase intracellular Ca^{2+} levels[13], triggering the activation of CAMKK2 and CAMKK2-mediated phosphorylation and activation of AMPK[32].

G_q-mediated inhibition of lipolysis in mouse GqD-3T3F442A adipocytes

We carried out additional studies to explore the signaling pathway(s) mediating GqD-mediated inhibition of lipolysis. Treatment of GqD-3T3F442A adipocytes with CL316,243 (100 nM) caused a pronounced increased in lipolysis, as determined by the amount of glycerol secreted into the medium (Fig. 4f). The lipolytic effect of CL316,243 is known to be primarily due to G_s-mediated activation of PKA[33]. The lipolytic response to CL316,243 was greatly reduced by co-incubation of GqD-3T3F442A cells with CNO (10 µM) (Fig. 4f). The ability of CNO to inhibit CL316,243-induced lipolysis was abolished by treatment of cells with FR900359 (1 µM) (Fig. 4g), confirming that CNO counteracts G_s-stimulated lipolysis by activating G_q-dependent signaling in GqD-3T3F442A cells. In addition, pharmacological blockade of CAMKK2 by STO-609 (2 µM) or inhibition of AMPK by Compound C (10 µM) abolished the ability of CNO-activated GqD receptors to reduce CL316,243-stimulated lipolysis in GqD-3T3F442A cells (Fig. 4h, i). CNO (10 µM) treatment of GFP-3T3F442A control cells had no significant effect on CL316,243-induced lipolysis (Supplementary Fig. 4d, e). These observations are in agreement with the data shown in Fig. 3, indicating that GqD-mediated activation of AMPK leads to the phosphorylation of HSL at a site that inhibits HSL activity.

Consistent with the in vitro data, CNO treatment (10 mg/kg i.p.) of adipo-GqD mice, but not of control littermates, caused a significant decrease of plasma FFA levels in vivo (Fig. 4j). Moreover, while CL316,243 (0.1 µg/kg i.p.) caused a ~2-fold increase in plasma FFA levels in control mice in vivo (Fig. 4k), this stimulatory CL316,243 response was absent in adipo-GqD mice treated with a mixture of CL316,243 and CNO (Fig. 4k). These findings further corroborate the concept that activation of adipocyte G_q signaling counteracts G_s-stimulated lipolysis.

Studies with differentiated human adipocytes

We next examined whether the metabolic effects observed after activation of adipocyte G_q signaling in mice are also conserved in human adipocytes. Specifically, we carried out glucose uptake and lipolysis assays with immortalized, differentiated human white adipocytes (hWAT cells)[34] infected with an adenovirus coding for GqD (GqD-hWAT cells). As observed with mouse adipocytes, CNO (10 µM) treatment of GqD-hWAT cells caused a significant increase in glucose uptake (Fig. 5a). This stimulatory CNO effect was abolished by treatment of GqD-hWAT cells with FR900359 (1 µM), BAPTA (10 µM), or Compound C (10 µM) (Fig. 5a), indicating that activation of G_q signaling promotes glucose uptake via a similar mechanism in mouse and human adipocytes.

While the β3-AR is the predominant β-AR subtype in mouse adipocytes[35], human adipocytes primarily express β1- and β2-ARs[36]. Treatment of differentiated GqD-hWAT cells with isoproterenol (100 nM), a non-subtype-selective β-AR agonist, led to a significant stimulation of lipolysis (Fig. 5b). This isoproterenol effect was absent in GqD-hWAT cells treated with a mixture of isoproterenol (100 nM) and CNO (10 µM) (Fig. 5b). CNO was unable to inhibit isoproterenol-stimulated lipolysis in GqD-hWAT cells in the presence of FR900359 (1 µM), STO-609 (2 µM), or Compound C (10 µM) (Fig. 5b). These data indicate that receptor-mediated activation of G_q signaling inhibits lipolysis in both mouse and human adipocytes via a CAMKK2/AMPK-dependent pathway.

Studies with primary mouse adipocytes lacking AMPK

To demonstrate in a more direct fashion that AMPK is required for G_q-mediated glucose uptake and inhibition of lipolysis, we carried out additional assays with primary mouse adipocytes (differentiated from pre-adipocytes) lacking AMPK. Specifically, we prepared
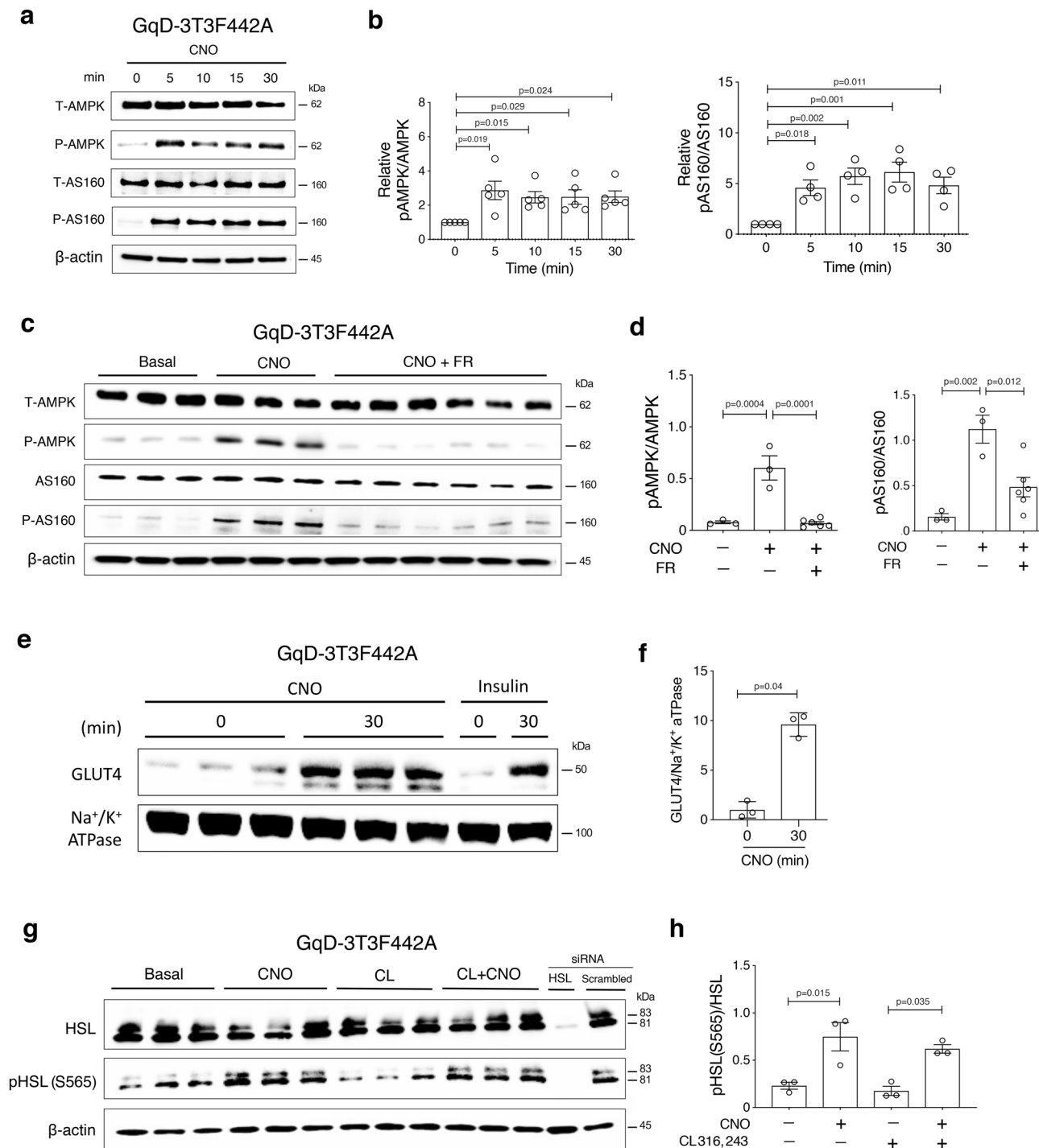
Fig. 3 Gq-mediated stimulation of AMPK phosphorylation, GLUT4 translocation, and phosphorylation of HSL (S565) in 3T3F442A mouse adipocytes.
a Western blotting studies with GqD-expressing mouse 3T3F442A cells (GqD-3T3F442A cells) treated with CNO (10 μM) for different periods of time.
b Quantitative analysis of pAMPK/AMPK and pAS160/AS160 protein expression levels shown in (**a**). Data shown in (**b**) were derived from four of five independent experiments. Protein expression levels were normalized relative to protein expression levels at time '0'. **c** Western blotting studies carried out in the presence of a $G_{q/11}$ inhibitor. GqD-3T3F442A cells) were incubated with CNO (10 μM) for 30 min either in the absence or presence of FR900359 (FR; 1 μM), a $G_{q/11}$ inhibitor. **d** Quantitative analysis of pAMPK/AMPK and pAS160/AS160 protein expression levels shown in (**c**). **e** Immunoblotting analysis of GLUT4 plasma membrane localization. After treatment of GqD-3T3F442A cells with CNO (10 μM) or insulin (10 nM) for 30 min, the plasma membrane fraction was isolated and subjected to immunoblotting analysis using an anti-GLUT4 antibody. Na + /K + ATPase served as a marker for plasma membrane proteins. **f** Quantitative analysis of GLUT4 expression levels shown in (**e**). **g** Western blot analysis of HSL phosphorylation at position S565. GqD-3T3F442A cells were treated with CNO (10 μM), CL316,243 (CL; 100 nM), a β3-adrenergic receptor agonist, or a combination of both drugs. To demonstrate the specificity of the HSL antibody used, GqD-3T3F442A cells were treated with HSL-specific siRNA or scrambled control siRNA.
h Quantitative analysis of pHSL(S565)/HSL protein expression levels shown in (**g**). Data are presented as means ± s.e.m. **b**, **d**, **f**, **h**: one-way ANOVA followed by Bonferroni's post-hoc test). Source data are provided as a Source data file.
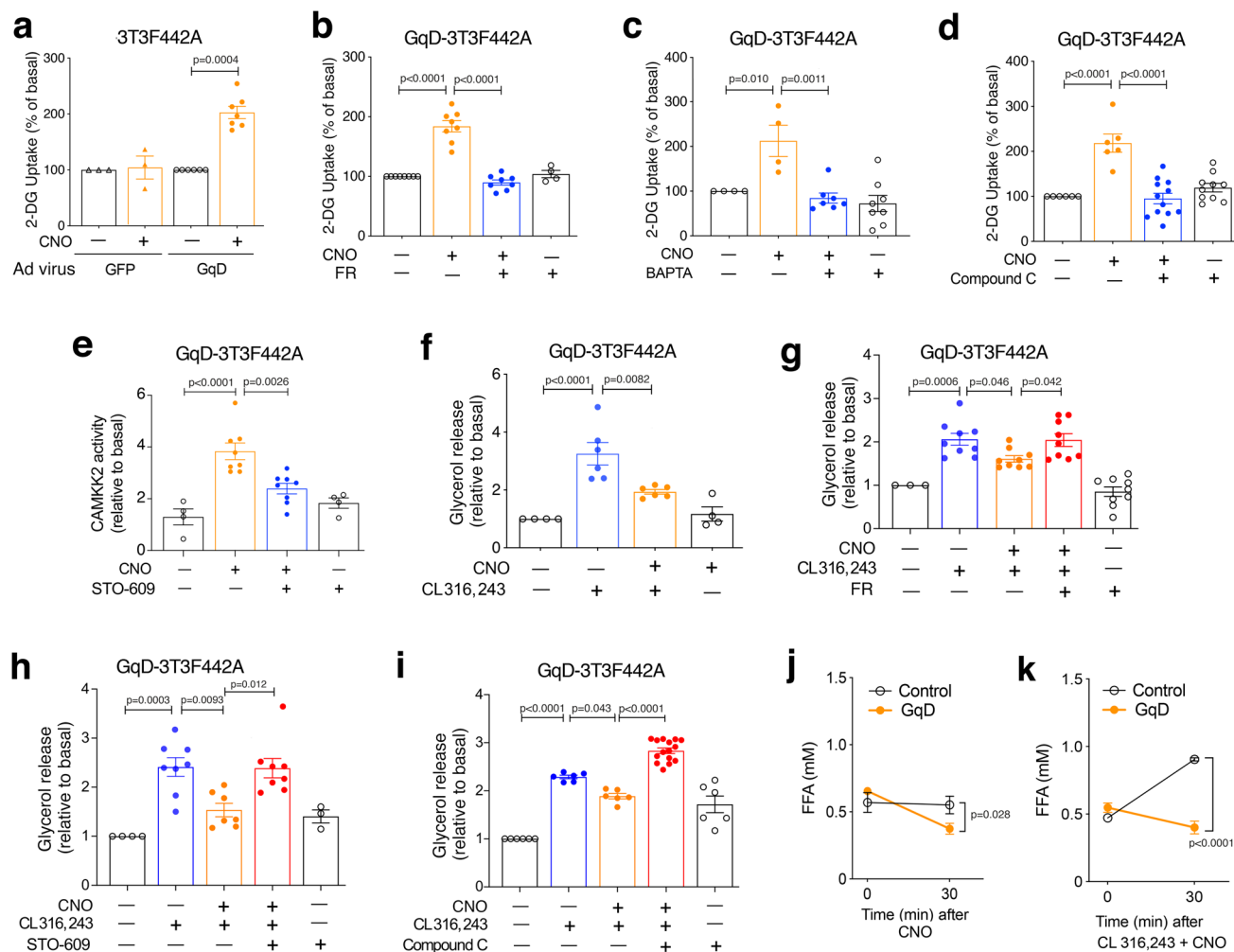
Fig. 4 Activation of G_q signaling promotes glucose uptake and inhibits lipolysis in 3T3F442A adipocytes. a ^{14}C-2-Deoxy-D-glucose (2-DG) uptake in GFP- or GqD-expressing 3T3F442A cells after treatment with CNO (10 μM). **b–d,** 2-DG uptake by CNO (10 μM)-treated GqD-expressing 3T3F442A cells in the presence or absence of the $G_{q/11}$ inhibitor FR900359 (FR; 1 μM) (**b**), BAPTA (Ca^{2+} chelator, 10 μM) (**c**), or Compound C (AMPK inhibitor, 10 μM) (**d**). **e** CAMKK2 activity of GqD-expressing 3T3F442A cells after treatment with CNO (10 μM) and/or STO-609 (CAMKK2 inhibitor, 2 μM). **f** Glycerol release after treatment of GqD-expressing 3T3F442A cells with CL316,243 (100 nM) in the presence or absence of CNO (10 μM). **g–i** Glycerol release after treatment of GqD-expressing 3T3F442A cells with CL316,243 (100 nM), CNO (10 μM), and various pharmacological inhibitors (**g**: FR, 1 μM; **h**: STO-609, 2 μM; **i**: Compound C, 10 μM).). **j** Plasma FFA levels in adipo-GqD (GqD) and control mice before and after acute CNO injection (10 mg/kg i.p.) ($n = 4$-8 per group). **k** Plasma FFA levels in adipo-GqD (GqD) and control mice before and after i.p. treatment with CL316,243 (0.1 μg/kg) plus CNO (10 mg/kg) ($n = 8$ per group). In (**a–i**), data were normalized relative to values obtained in the absence of any drugs. Data are presented as means ± s.e.m. of at least three independent experiments (**a–i**). **a**, **j**, **k**: two-tailed Student's t-test; **b–i**: one-way ANOVA followed by Bonferroni's post-hoc test). Source data are provided as a Source data file.

adipocytes (pre-adipocytes) from iWAT of *adipoq-CreER^T2^-AMPK β1^flox/flox^β2^flox/flox^* mice[37] in which the two β subunits of AMPK were deleted by tamoxifen treatment[37]. Subsequently, the adipocytes were infected with an adenovirus encoding GqD. Since the β1 and β2 subunits are essential for AMPK heterotrimer formation, the absence of the two β subunits also resulted in a nearly complete loss of the expression of AMPKα, including its active form, p(T172)-AMPKα[37] (Fig. 5c). For the sake of simplicity, we refer to these AMPK-deficient, GqD-expressing adipocytes simply as GqD-AMPK-KO adipocytes.

In agreement with the analysis of GqD-expressing 3T3-F442A adipocytes (Fig. 4a–d), CNO (10 μM) treatment of GqD-expressing primary adipocytes (differentiated from preadipocytes) prepared from control mice led to a ~2-fold increase in glucose uptake, an effect that could be completely blocked by pharmacological inhibition of CAMKK2 by STO-609 (2 μM) (Fig. 5d). In contrast, CNO was unable to stimulate glucose uptake in GqD-AMPK-KO

adipocytes (Fig. 5d), providing additional strong evidence that G_q-mediated activation of glucose uptake in adipocytes requires the presence of AMPK.

Lipolysis assays showed that CNO (10 μM) treatment of GqD-primary adipocytes inhibited the increase in lipolysis caused by CL316,243 (100 nM)-induced activation of β3-ARs (Fig. 5e). This CNO effect was completely absent after STO-609 (2 μM)-mediated inhibition of CAMKK2 (Fig. 5e). These findings mirror the data obtained with GqD-expressing 3T3-F442A adipocytes (Fig. 4f–i). Importantly, CNO treatment failed to inhibit CL316,243-induced lipolysis in GqD-AMPK-KO adipocytes (Fig. 5e). This observation further corroborates the concept that G_q-mediated inhibition of lipolysis requires the activity of AMPK.

Metabolic studies with mutant mice lacking $Gα_{q/11}$ selectively in adipocytes. The α-subunits of G_q and G_{11} ($Gα_q$ and $Gα_{11}$,
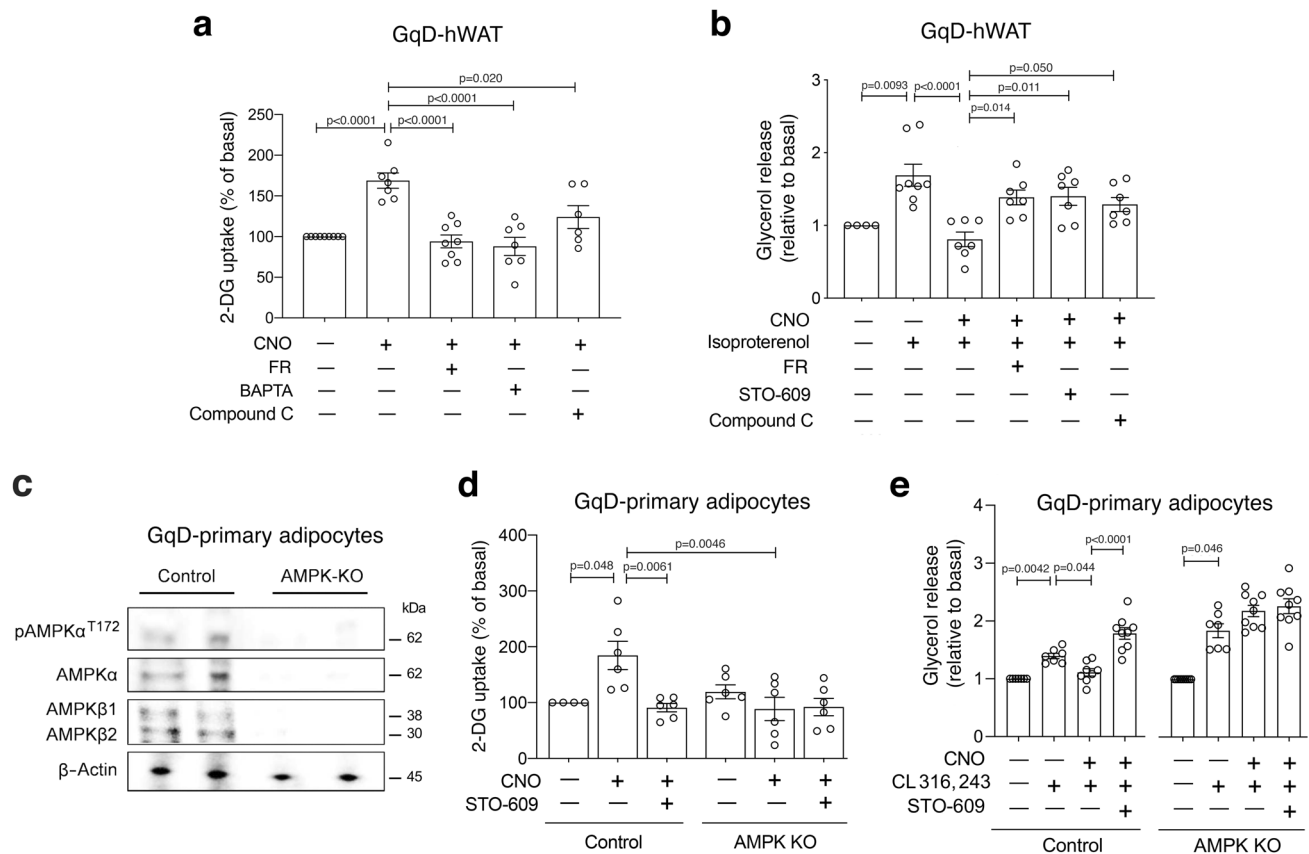
Fig. 5 Studies with human adipocytes and primary mouse adipocytes lacking AMPK. a 2-Deoxy-D-glucose (2-DG) uptake by CNO (10 μM)-treated GqD-expressing, differentiated human white adipocytes (GqD-hWAT cells) in the presence or absence of FR900359 (FR; 1 μM), (BAPTA (10 μM), and Compound C (10 μM). **b** Glycerol release after treatment of GqD-hWAT cells with isoproterenol (100 nM), CNO (10 μM), and various pharmacological inhibitors (FR, 1 μM; STO-609, 2 μM; Compound C, 10 μM). **c** Western blot analysis with GqD-expressing primary mouse adipocytes (source: iWAT) demonstrating the lack of all three subunits of AMPK in AMPK KO cells (control = GqD-expressing primary mouse adipocytes with functional AMPK). This experiment was independently repeated twice with similar results. **d** 2-DG uptake by CNO (10 μM)-treated GqD-expressing primary mouse adipocytes in the presence (control) or absence of AMPK (AMPK KO), either with or without STO-609 (2 μM) co-incubation. **e** Glycerol release from CNO (10 μM)-treated GqD-expressing primary mouse adipocytes in the presence (control) or absence of AMPK (AMPK KO). Lipolysis was induced by incubation with CL316,243 (100 nM). Experiments were carried out in the absence or presence of STO-609 (2 μM). Glucose uptake and glycerol release data were normalized relative to values obtained in the absence of any drugs. Data are presented as means ± s.e.m. of at least four independent experiments. **a**, **b**, **d**, **e**: one-way ANOVA followed by Bonferroni's post-hoc test). Source data are provided as a Source data file.

respectively) are structurally closely related and have similar functional roles[13]. $G\alpha_q$ and $G\alpha_{11}$ are co-expressed in virtually all cell types including adipocytes[13]. Whole-body $G\alpha_q$ knockout (KO) mice display multiple peripheral and central deficits, while whole-body $G\alpha_{11}$ KO mice appear phenotypically normal[13]. To explore the role of $G_{q/11}$ signaling in different cell types in vivo, Wettschureck et al. previously generated $G\alpha_q flox/flox$ $G\alpha_{11} -/-$ mice[38]. By crossing these mutant mice with *adipoq-Cre* mice, we obtained mutant mice lacking $G_{q/11}$ in adipocytes (adipo-$G_{q/11}$ KO mice) (Fig. 6a).

H&E staining of iWAT, eWAT, and BAT sections from adipo-$G_{q/11}$ KO mice and control littermates did not reveal any obvious genotype-dependent morphological differences (Supplementary Fig. 7a). Moreover, the weights of different adipose tissue depots (expressed as % of body weight) did not differ significantly between the two groups of mice (Supplementary Fig. 7b).

Adipo-$G_{q/11}$ KO mice did not differ from their control littermates ($G\alpha_q flox/flox$ $G\alpha_{11} -/-$ mice lacking the *adipoq-Cre* transgene) in body weight and composition (% fat and % lean mass), fed and fasting blood glucose and plasma insulin and leptin levels, as well as insulin sensitivity measured in an insulin tolerance test (Fig. 6b, c, e-h). However, adipo-$G_{q/11}$ KO mice displayed significantly impaired glucose tolerance (Fig. 6d), as

well as increased fasting plasma FFA and glycerol levels, as compared to their control littermates (Fig. 6i, j).

To induce obesity-associated metabolic deficits, we maintained adipo-$G_{q/11}$ KO mice and their control littermates on a HFD for 8 weeks (Supplementary Fig. 8a). We found that HFD adipo-$G_{q/11}$ KO mice showed significantly higher fasting blood glucose and plasma FFA levels than HFD control mice (Supplementary Fig. 8b, c). Moreover, glucose tolerance was severely impaired in HFD adipo-$G_{q/11}$ KO mice, as compared to HFD control littermates (Supplementary Fig. 8f). Taken together, these observations clearly indicate that signaling via $G_{q/11}$ proteins endogenously expressed by adipocytes plays a physiological role in maintaining proper glucose and lipid homeostasis.

Insulin action is not affected by the lack of adipocyte $G_{q/11}$ signaling. Previously published data involving the use of cultured 3T3-L1 cells suggested that G_q-mediated signaling is involved in mediating insulin-induced effects[39]. To further explore this link, we injected adipo-$G_{q/11}$ KO mice and control littermates (*Gaq-flox/flox Ga11 -/-* mice lacking the *adipoq-Cre* transgene) with insulin (0.75 U /kg i.p.), followed by the measurement of blood glucose and plasma FFA levels 30 min later. We found that
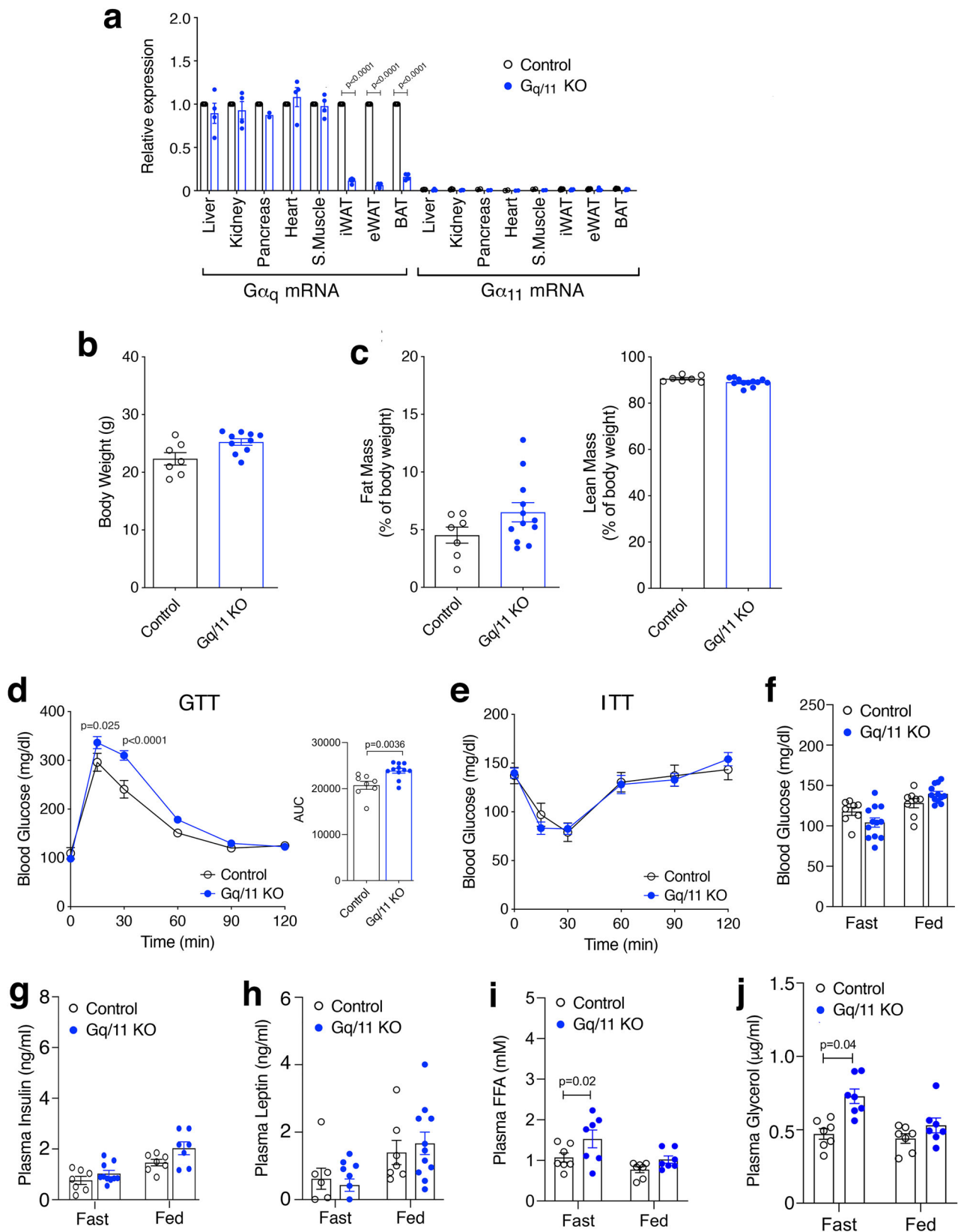
insulin treatment reduced blood glucose and plasma FFA levels to a similar degree in control and adipo-$G_{q/11}$ KO mice (Supplementary Fig. 9a, b). Moreover, studies with 3T3F442A cells showed that the ability of insulin (10 nM) to stimulate glucose uptake and inhibit β3-adrenergic receptor (CL316,243)-mediated lipolysis was not significantly different in the presence or absence of FR900359 (FR; $G_{q/11}$ inhibitor; 1 µM) (Supplementary Fig. 9c, d). Taken together, our data suggest that insulin action on adipocytes does not require the presence of adipocyte $G_{q/11}$ under our experimental conditions.

Fig. 6 Adipocyte-selective G$_{q/11}$ KO mice show deficits in blood glucose and lipid homeostasis. a Expression levels of $G\alpha_q$ and $G\alpha_{11}$ mRNA in different tissues of adipo-G$_{q/11}$ KO mice and control littermates ($G\alpha_q$flox/flox $G\alpha_{11} -/-$ mice lacking the *adipoq-Cre* transgene) ($n = 4$ per group). Transcript levels were normalized relative to $G\alpha_q$ mRNA levels of control mice (set equal to 1). **b, c** Body weight (**b**) and body composition (fat and lean mass as % of body weight) (**c**) of adipo-G$_{q/11}$ KO mice and control littermates (mouse age: 12 weeks; $n = 7$–12 per group). **d, e** GTT (**d**; the panel to the right shows AUC values) and ITT (**e**) of adipo-G$_{q/11}$ KO mice and control littermates. Blood glucose levels were measured after i.p. injection of 2 g/kg glucose after overnight fasting (**d**) or of 0.75 U/kg insulin after a 4 hr fast (**e**), respectively ($n = 8$–13 per group). **f–i**, Blood glucose (**f**), and plasma insulin (**g**), leptin (**h**), FFA (**i**), and glycerol (**j**) levels of adipo-G$_{q/11}$ KO and control mice under fasting and fed conditions ($n = 7$–12 per group). Data are presented as means ± s.e.m. **d**, **e**: two-way ANOVA followed by Bonferroni's post-hoc test; **a**, **f–j**: two-tailed Student's t-test). Source data are provided as a Source data file.

G$_q$-coupled receptors endogenously expressed by adipocytes. Since activation or disruption of G$_q$ signaling in adipocytes had significant effects on glucose uptake and lipolysis, we speculated that targeting G$_q$-coupled receptors endogenously expressed by adipocytes might prove beneficial to treat impairments in glucose and lipid homeostasis. We recently subjected RNA prepared from isolated mouse adipocytes (iWAT and eWAT) to RNA-seq analysis[14]. This analysis demonstrated that mouse adipocytes express several GPCRs that are selectively coupled to G$_{q/11}$, including the P2Y$_6$ receptor, the complement component 5a receptor 1, the cysteinyl leukotriene receptors 1 and 2, and several orphan GPCRs (Supplementary Table 1). Interestingly, the expression levels of several of these receptors were upregulated when mice were maintained on a HFD (Supplementary Table 1).

Amisten et al.[11] recently published a comprehensive list of GPCRs expressed by human subcutaneous fat (abdominal and gluteofemoral fat depots). The most abundantly expressed G$_q$-coupled receptors for which quantitative expression data were provided are listed in Supplementary Table 2. A comparison of the receptors listed in Supplementary Tables 1 and 2 indicates that the cysteinyl leukotriene receptor 2 (CysLT$_2$ receptor) is expressed in both mouse adipocytes and in human subcutaneous fat.

CysLT$_2$ receptor function in human adipocytes. We next studied the potential functional roles of the CysLT$_2$ receptor in human adipocytes. Fig. 7a shows that CysLT$_2$ receptor expression (mRNA levels) dramatically increases during the differentiation of human white adipocytes (hWAT cells). Moreover, studies with lean human subjects and individuals with obesity demonstrated that CysLT$_2$ receptor transcript levels in subcutaneous fat from biopsy samples[40] correlated well with body mass index (BMI) and fat mass (% of body weight) (Fig. 7b, c), suggesting that adipocyte CysLT$_2$ receptors may play a role in regulating the function of human WAT.

To further explore this concept, we treated differentiated hWAT cells with N-methyl leukotriene C$_4$ (NMLTC$_4$), a selective CysLT$_2$ receptor agonist[41]. NMLTC$_4$ is a metabolically more stable analog of leukotriene C$_4$ (LTC$_4$) and activates both mouse and human CysLT$_2$ receptors with high selectivity in vitro and in vivo[41]. Incubation of hWAT cells with NMLTC$_4$ (1 μM) led to a ~twofold increase in glucose uptake (Fig. 7d). The magnitude of this effect was similar to that observed after treatment of hWAT cells with insulin (10 nM) (Fig. 7d). The NMLTC$_4$-stimulated increase in glucose uptake could be blocked by HAMI3379 (1 μM), a potent and selective blocker of CysLT$_2$ receptors[42], as well as FR900359 (1 μM), indicating that activation of human adipocyte CysLT$_2$ receptors promotes glucose uptake via stimulation of G$_{q/11}$ signaling (Fig. 7d).

Studies with differentiated hWAT cells also showed that NMLTC$_4$ (1 μM) effectively inhibited the increase in lipolysis caused by isoproterenol (100 nM), a nonsubtype-selective β-AR agonist (Fig. 7e). This inhibitory NMLTC$_4$ effect was not observed in the presence of the CysLT$_2$ receptor antagonist, HAMI3379 (1 μM), or the G$_{q/11}$ inhibitor, FR900359 (1 μM)

(Fig. 7e). These findings clearly indicate that adipocyte CysLT$_2$ receptors mediate inhibition of lipolysis in human adipocytes via activation of G$_{q/11}$ signaling.

In agreement with the data obtained with CNO-treated, GqD-expressing mouse adipocytes (Fig. 3a, b), NMLTC$_4$ treatment of hWAT cells also efficiently promoted the phosphorylation of AMPK (Fig. 7f).

Activation of adipocyte G$_q$ signaling overcomes metabolic deficits caused by adipocyte insulin receptor deficiency. It is known that insulin resistance of adipose tissue plays a key role in the pathogenesis of T2D[43]. In agreement with this concept, mutant mice lacking insulin receptors (IRs) selectively in adipocytes develop profound insulin resistance and hyperglycemia[44]. Our in vitro data obtained with cultured mouse and human adipocytes indicated that receptor-mediated activation of G$_{q/11}$ was able to stimulate glucose uptake and inhibit lipolysis by adipocytes in an insulin-independent fashion. We therefore hypothesized that activation of adipocyte G$_{q/11}$ signaling might compensate for impaired insulin signaling in adipocytes. To test this hypothesis, we generated adipo-GqD mice that carried only one copy of the IR gene in adipocytes (adipo-GqD-IR$^{+/-}$ mice; heterozygous, adipocyte-specific IR KO mice expressing GqD in adipocytes). As shown in Supplementary Fig. 10, the expression of IR mRNA was reduced by ~50% in adipose tissues isolated from adipo-GqD-IR$^{+/-}$ mice, as compared to their control littermates (LSL-GqD-IR$^{+/flox}$ mice that do not carry the *adipoq-Cre* transgene).

When maintained on a HFD, adipo-GqD-IR$^{+/-}$ mice showed similar body weight gain as their control littermates (Fig. 8a). However, after 8 weeks of HFD feeding, adipo-GqD-IR$^{+/-}$ mice displayed a significant reduction in body fat mass, accompanied by a significant increase in lean mass (Fig. 8b). Although plasma insulin levels were increased in fasted adipo-GqD-IR$^{+/-}$ mice (Fig. 8c), fasting blood glucose and plasma FFA levels were significantly elevated in adipo-GqD-IR$^{+/-}$ mice (Fig. 8d, e), indicating that reduced IR signaling in adipocytes causes impaired glucose and lipid homeostasis. To investigate whether activation of adipocyte G$_q$ signaling was able to ameliorate these metabolic deficits, we injected HFD adipo-GqD-IR$^{+/-}$ mice and their control littermates with a single i.p. dose of CNO (10 mg/kg) or vehicle (saline). Vehicle-treated adipo-GqD-IR$^{+/-}$ mice showed a pronounced increase in blood glucose levels, most likely due to stress-induced glucose mobilization (Fig. 8f). This effect was not observed when adipo-GqD-IR$^{+/-}$ mice received CNO instead of vehicle (Fig. 8f). Plasma insulin levels remained largely unchanged in adipo-GqD-IR$^{+/-}$ and control mice after vehicle or CNO administration (Fig. 8g). Strikingly, CNO treatment of adipo-GqD-IR$^{+/-}$ mice, but not of control littermates, led to a pronounced reduction in plasma FFA and glycerol levels (Fig. 8h, i), indicating that activation of adipocyte G$_{q/11}$ signaling inhibits lipolysis in this mouse model of insulin resistance. As expected, this CNO effect was not observed with control mice that did not express the GqD designer receptor (Fig. 8h, i).
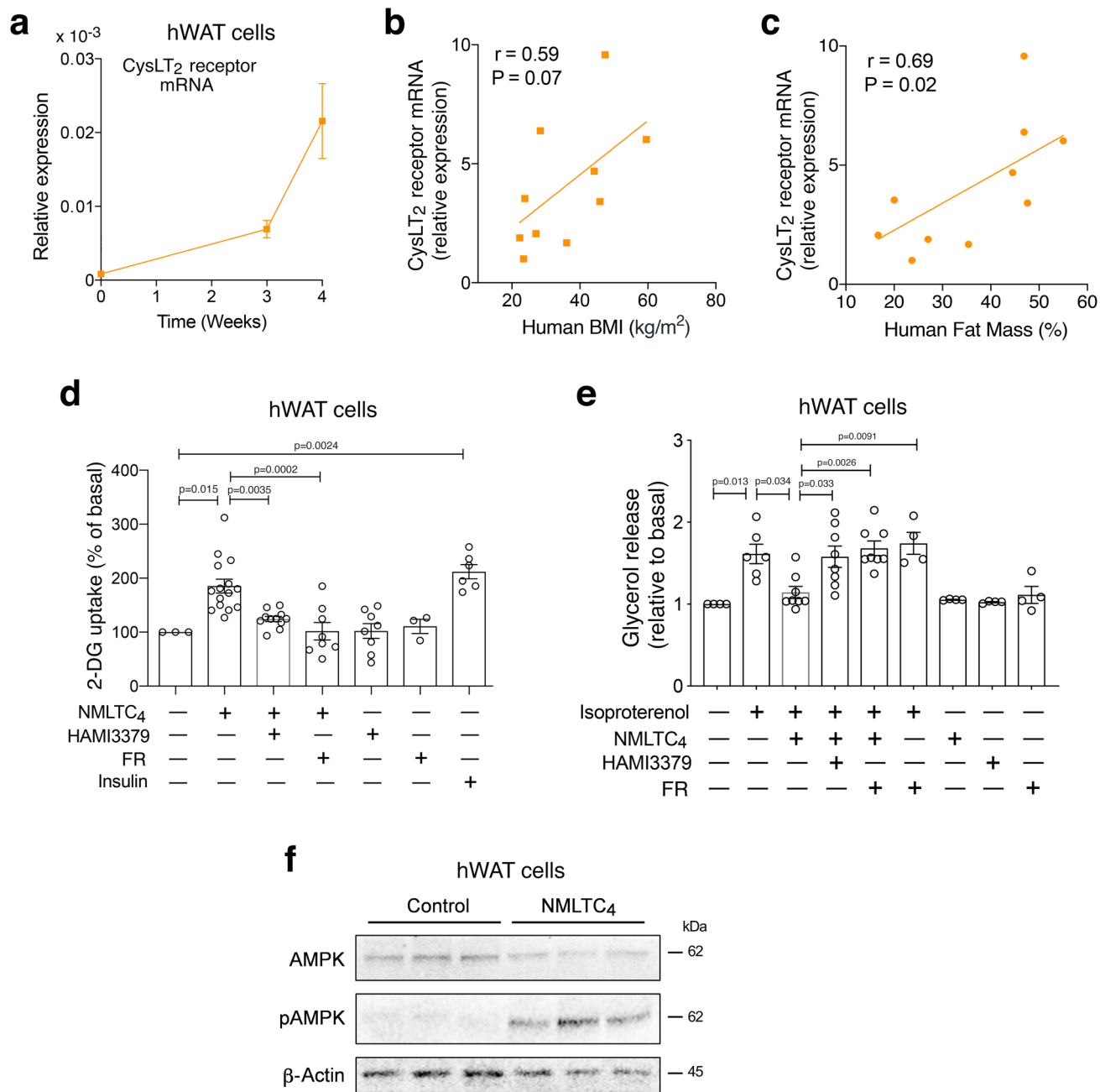
Fig. 7 Agonist stimulation of the CysLT$_2$ receptor promotes glucose uptake and inhibits lipolysis in human white adipocytes. a Changes in mRNA levels of the CysLT$_2$ receptor during the differentiation of human white adipocytes (hWAT cells). **b** Correlation between human body mass index (BMI) and CysLT$_2$ receptor mRNA expression levels in human subcutaneous fat ($n = 10$; samples were from 10 different individuals). **c** Correlation between human fat mass (% of body weight) and CysLT$_2$ receptor mRNA expression levels in human subcutaneous fat ($n = 10$; samples were from 10 different individuals). **d** Stimulation of 2-deoxy-D-glucose (2-DG) uptake by differentiated hWAT cells by NMLTC$_4$, a selective CysLT$_2$ receptor agonist (1 μM). HAMI3379, a selective CysLT$_2$ receptor antagonist (1 μM) and FR900359 (FR; G$_{q/11}$ inhibitor; 1 μM) blocked this response. For control purposes, cells were also treated with insulin (10 nM). **e** Stimulation of glycerol release from differentiated hWAT cells by isoproterenol (100 nM). This effect was completely blocked by NMLTC$_4$ (1 μM). The anti-lipolytic effect of NMLTC$_4$ was absent in the presence of HAMI3379 (1 μM) or FR (1 μM). Glucose uptake and glycerol release data were normalized relative to values obtained in the absence of any drugs. **f** Western blotting studies with differentiated hWAT cells. Treatment with NMLTC$_4$ (1 μM) for 60 min promotes the phosphorylation of AMPK (α-subunit). This experiment was independently repeated twice with similar results. The correlation analysis shown in (**b**, **c**) was conducted by Spearman's test (two-tailed, no adjustment for multiple comparisons). The data shown in (**a**, **d**, **e**) are means ± s.e.m. obtained in at least three independent experiments. In (**d**, **e**), data were expressed relative to basal levels measured in the absence of any drugs (one-way ANOVA followed by Bonferroni's post-hoc test). Source data are provided as a Source data file.
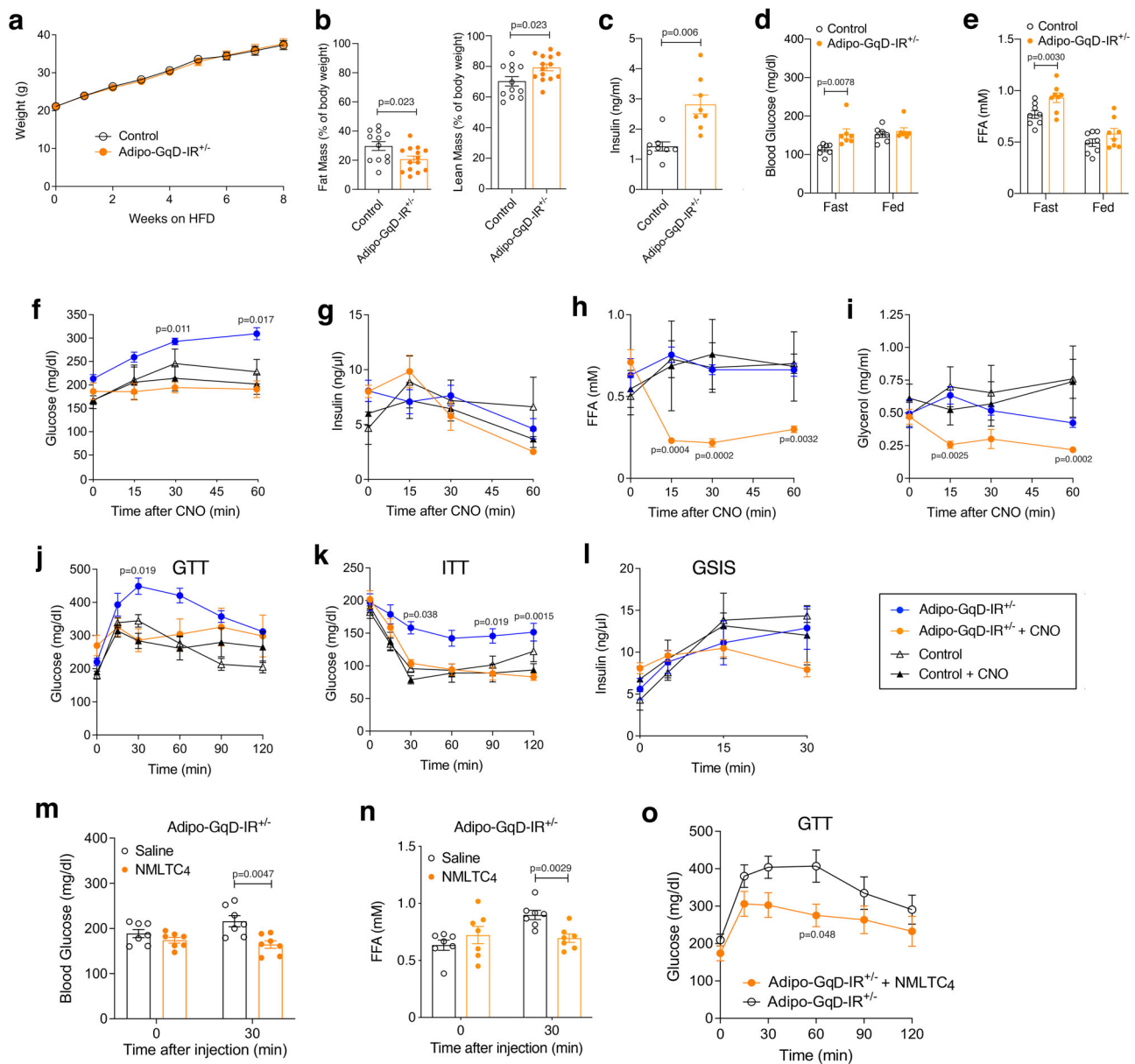
Fig. 8 Activation of adipocyte G_q signaling restores normal glucose and lipid homeostasis in adipocyte-specific insulin receptor (IR) mutant mice. a Body weight gain of adipo-GqD-IR$^{+/-}$ mice (adipocyte-specific heterozygous insulin receptor knockout mice expressing GqD in adipocytes) and control littermates (LSL-GqD-IR$^{+/flox}$ mice that do not carry the *adipoq-Cre* transgene) maintained on a high fat diet (HFD). **b–e** Body composition (fat and. lean body mass) (**b**), plasma insulin levels after a 16 hr overnight fast (**c**), and fed and fasting (16 hr overnight) blood glucose (**d**) and plasma FFA levels (**e**) of adipo-GqD-IR$^{+/-}$ mice and control littermates maintained on HFD for ~10 weeks. **f–i**, Blood glucose (**f**), plasma insulin (**g**), plasma FFA (**h**), and plasma glycerol (**i**) levels of HFD adipo-GqD-IR$^{+/-}$ and control mice after acute treatment with CNO (10 mg/kg i.p.) following a 4 hr fast. **j–l**, GTT (**j**), ITT (**k**), and GSIS (**l**) performed with HFD adipo-Gq-IR$^{+/-}$ mice and control littermates with or without CNO (10 mg/kg i.p.) treatment. In (**j**), mice were injected with 1 g/kg glucose (i.p.) after a 4 h fast. In (**k**) and (**l**), mice that had been fasted for 4 hr received 1 U/kg insulin (i.p) or a bolus of glucose (1 g/kg i.p.), respectively. **m–o**, NMLTC$_4$ treatment of HFD adipo-GqD-IR$^{+/-}$ mice. **m**, **n**, Blood glucose (**m**) and plasma FFA (**n**) levels of HFD adipo-GqD-IR$^{+/-}$ mice after treatment with NMLTC$_4$ (10 μg/kg) or saline following a 4 h fast. **o**, GTT. After a 4 h fast, HFD adipo-GqD-IR$^{+/-}$ mice were injected with glucose (1 g/kg i.p.), either in the presence or absence of NMLTC$_4$ (10 μg/kg). All experiments were carried out with male mice maintained on HFD for 8–14 weeks Data are presented means ± s.e.m. (**a**, **b**: n = 10-14 per group; **c–o**: n = 5-8 per group). **b–e**, **m**, **n**: two-tailed Student's *t*-test; **f–l**, **o**: two-way ANOVA followed by Bonferroni's post hoc test) (**f–l**: adipo-GqD-IR$^{+/-}$ plus CNO vs. adipo-GqD-IR$^{+/-}$ without CNO). Source data are provided as a Source data file.

HFD adipo-GqD-IR$^{+/-}$ mice also showed significant impairments in glucose tolerance and peripheral insulin sensitivity, as compared with their HFD control littermates (Fig. 8j, k). Notably, co-administration of glucose (1 g/kg i.p.) or insulin (1 U/kg i.p.) with CNO (10 mg/kg i.p.) greatly improved glucose tolerance and insulin sensitivity caused by the relative lack of IRs in adipocytes (Fig. 8j, k). Expectedly, CNO administration had no significant effect on glucose tolerance and insulin sensitivity in HFD control

littermates (Fig. 8j, k). Administration of a glucose bolus (1 g/kg i.p.) triggered comparable increases in plasma insulin levels in adipo-GqD-IR$^{+/-}$ and control mice, either in the presence or absence of co-injected after CNO (Fig. 8l).

Treatment with a CysLT$_2$ receptor agonist ameliorates the metabolic deficits displayed by adipo-GqD-IR$^{+/}$ mice. Since

$CysLT_2$ receptors are expressed in both mouse and human adipocytes/fat tissues (Supplementary Tables 1 and 2) and $NMLTC_4$, a selective $CysLT_2$ receptor agonist, promoted glucose uptake and inhibited lipolysis in cultured hWAT cells (Fig. 7d, e), we next injected HFD adipo-GqD-IR$^{+/−}$ mice with a single i.p. dose of $NMLTC_4$ (10 µg/kg i.p.) or vehicle (saline). Thirty minutes later, the $NMLTC_4$-treated adipo-GqD-IR$^{+/−}$ mice showed significantly decreased blood glucose and plasma FFA levels, as compared to the vehicle-treated adipo-GqD-IR$^{+/−}$ mice (Fig. 8m, n). Moreover, a GTT showed that co-administration of glucose (1 g/kg i.p.) with $NMLTC_4$ (10 µg/kg i.p.) greatly improved the deficit in glucose tolerance displayed by HFD adipo-GqD-IR$^{+/−}$ mice (Fig. 8o).

The beneficial metabolic effects caused by $CysLT_2$ receptor activation require adipocyte $G_{q/11}$ signaling. To explore whether the beneficial metabolic effects caused by $NMLTC_4$ treatment were mediated by adipocyte $G_{q/11}$ signaling, we next injected HFD adipo-$G_{q/11}$ KO and control mice with either vehicle (saline) or $NMLTC_4$ (10 µg/kg i.p.). Injection with saline caused modest increases in blood glucose and plasma FFA levels in most mice (Supplementary Fig. 8d, e), most likely due to the injection stress. Injection of HFD adipo-$G_{q/11}$ KO mice with $NMLTC_4$ (10 µg/kg i.p.) resulted in similar responses (Supplementary Fig. 8d, e). In contrast, $NMLTC_4$ treatment of HFD control mice did not cause increases in blood glucose and plasma FFA levels in most animals, suggesting that activation of adipocyte CysLT2 receptors counteracts the increases in blood glucose and plasma FFA levels caused by the injection stress.

Importantly, while $NMLTC_4$ treatment significantly improved glucose tolerance in HFD control mice, $NMLTC_4$ had no effect on the severe impairment in glucose tolerance displayed by HFD adipo-$G_{q/11}$ KO mice (Supplementary Fig. 8f, g). Taken together, these data indicate that the beneficial metabolic effects of $NMLTC_4$ treatment were mediated by adipocyte CysLT2 receptors linked to the activation of $G_{q/11}$.

$G_{q/11}$ signaling is elevated in adipose tissue-derived from fasted mice. To explore whether fasting affected the degree of $G_{q/11}$ signaling in adipose tissues, we measured inositol monophosphate (IP_1) levels in adipose tissues isolated from freely fed and fasted (overnight for 14 hr) male WT C57BL/6 mice (age: 8 weeks). Mice consuming regular chow were injected with LiCl (10 mmoles/kg, s.c.), an inhibitor of IP_1 phosphatase, prior to the beginning of the dark cycle (6 pm). In the presence of LiCl, the intracellular accumulation of IP_1 is considered a good measure of the degree of $G_{q/11}$ signaling[45].

We found that fasted mice showed ~2.7-fold higher IP_1 levels in visceral fat (eWAT), as compared to mice that had free access to food (Supplementary Fig. 11). IP_1 levels also trended to be increased in subcutaneous fat (iWAT), but this effect failed to reach statistical significance (Supplementary Fig. 11). One possible explanation for this latter observation is that $G_{q/11}$-coupled receptors are expressed at lower levels in iWAT than in eWAT. In any case, the eWAT data support the concept that $G_{q/11}$ signaling is elevated in adipocytes under fasting conditions.

Discussion

Adipocyte function is regulated by many hormones, neurotransmitters, and signaling proteins, including GPCRs. Adipocytes express dozens of GPCRs that are linked to different functional classes of G proteins[11,12]. Previous in vivo studies have shown that selective activation of adipocyte G_s signaling leads to striking improvements in glucose homeostasis and protects mice from the metabolic deficits associated with the consumption of an obesogenic diet (see, for example, ref. [15,16]). Mechanistic data indicated that these beneficial metabolic effects are due to the ability of adipocyte G_s signaling to stimulate lipolysis and energy expenditure and to inhibit food intake[15,16]. Moreover, a recent study demonstrated that adipocyte G_i signaling is essential for maintaining euglycemia and proper peripheral insulin sensitivity, primarily due to G_i-mediated suppression of lipolysis and the resulting reduction of plasma FFA levels[14].

In the present study, we provide strong evidence that drug-induced activation of adipocyte G_q signaling improves glucose homeostasis and peripheral insulin sensitivity under both physiological and pathophysiological conditions. By using a chemogenetic approach, we demonstrated that these beneficial metabolic effects could be observed after both acute and chronic activation of adipocyte G_q signaling (Figs. 1, 2; Supplementary Fig. 2).

In agreement with these findings, mice that lacked $G_{q/11}$ in adipose tissue (adipo-$G_{q/11}$ KO mice) showed significant impairments in glucose homeostasis, associated with elevated fasting plasma FFA levels (Fig. 6). Similar deficits were observed when adipo-$G_{q/11}$ KO mice were maintained on an obesogenic diet (Supplementary Fig. 8). These data clearly indicate that endogenous adipocyte $G_{q/11}$ signaling is required for maintaining euglycemia and normal plasma FFA levels. The precise physiological and pathophysiological roles of adipocyte $G_{q/11}$ signaling remain to be explored in future studies.

While CNO treatment of adipo-GqD mice resulted in a striking decrease in blood glucose levels (Fig. 2c), fed and fasting blood glucose levels were similar in adipo-$G_{q/11}$ KO and control mice consuming regular chow (Fig. 6f). This latter observation suggests that other signaling pathways can compensate for the lack of adipocyte $G_{q/11}$ to maintain euglycemia. However, when challenged with an obesogenic diet, adipo-$G_{q/11}$ KO showed significantly elevated fasting blood glucose levels (Supplementary Fig. 8b).

We also found that the G_q-coupled $CysLT_2$ receptor is enriched in mouse and human adipocytes (Fig. 7a, Supplementary Tables 1 and 2). In agreement with the data obtained with adipo-GqD mice, $NMLTC_4$, a selective $CysLT_2$ receptor agonist, inhibited lipolysis and increased glucose uptake in human adipocytes (Fig. 7d, e) and improved glucose and lipid homeostasis in a mutant mouse strain characterized by impaired insulin signaling in adipocytes (see next paragraph) (Fig. 8m-o).

$NMLTC_4$ treatment of HFD adipo-$G_{q/11}$ KO failed to improve glucose homeostasis (Supplementary Fig. 8f), strongly suggesting that the beneficial metabolic effects of $NMLTC_4$ administration were mediated by adipocyte CysLT2 receptors linked to the activation of $G_{q/11}$. Thus, this proof-of-concept study indicates that agonist activation of a G_q-coupled receptor endogenously expressed by mouse and human adipocytes can lead to striking improvements in glucose homeostasis and other beneficial metabolic effects. In this context, it should be noted that gain of function mutations in the CysLT2 receptor are associated with various cancers (see, for example, ref. [46]). For this reason, it is unlikely that CysLT2 agonists can be developed for clinical use.

Studies with cultured mouse and human adipocytes indicated that agents able to activate adipocyte G_q signaling mimic the major actions of insulin on adipocyte function, inhibition of lipolysis, and stimulation of glucose uptake. In agreement with these observations, several previous studies reported that activation of G_q signaling can promote glucose uptake and/or GLUT4 translocation[39,47,48] and may inhibit lipolysis[49,50] in cultured adipocytes. On the basis of these findings, we speculated that drugs able to activate G_q signaling in adipocytes in vivo may prove useful to overcome impaired glucose and lipid homeostasis caused by adipose tissue insulin resistance. To test this

hypothesis, we generated insulin receptor (IR) mutant mice lacking one copy of the IR gene in adipocytes (adipo-IR^{+/−} mice). When maintained on an obesogenic diet (HFD), these mutant mice showed significantly increased fasting blood glucose and plasma FFA levels (despite increased plasma insulin levels), indicative of an insulin-resistant state (Fig. 8c-e). In agreement with these data, a recent study demonstrated that mutant mice lacking both copies of the IR gene selectively in adipocytes (adipo-IR^{−/−} mice) develop profound insulin resistance and hyperglycemia[44].

Remarkably, chemogenetic activation of G_q signaling in adipocytes of HFD adipo-GqD-IR^{+/−} mice greatly improved the deficits in glucose tolerance and insulin sensitivity displayed by the IR mutant mice (Fig. 8h-k). These data strongly support the concept that drugs that can stimulate G_q signaling in adipocytes, such as agonists acting on G_q-coupled receptors expressed by adipocytes, can overcome the metabolic deficits caused by impaired insulin action on adipose tissue. For this reason, our findings point to a new avenue to develop novel classes of anti-diabetic agents.

To study the molecular mechanism underlying the beneficial metabolic effects of activating G_q signaling in adipocytes, we carried out studies with cultured mouse and human adipocytes. CNO treatment of mouse and human adipocytes (hWAT cells) expressing the GqD designer receptor impaired lipolysis and improved glucose uptake (Figs. 4 and 5). Both effects were either completely abolished or greatly reduced after treatment with FR900359 (selective $G_{q/11}$ inhibitor), BAPTA (Ca^{2+} chelator), STO-609 (selective CAMKK2 inhibitor), and Compound C (selective AMPK inhibitor) (Figs. 4 and 5). Moreover, CNO was unable to promote glucose uptake and inhibit lipolysis in mouse primary adipocytes lacking AMPK (Fig. 5c-e), indicating that G_q-induced activation of AMPK plays a central role in mediating these effects. The ability of activated G_q to stimulate AMPK has also been observed in other tissues and cell types[51–53]. Following agonist binding, G_q-coupled receptors trigger increases in intracellular Ca^{2+} levels[10,13], leading to the activation of CAMKK2 which then phosphorylates and activates AMPK[32]. Activated AMPK is able to inhibit lipolysis via phosphorylation of HSL at S565, an event that interferes with proper HSL function (Fig. 3g, h)[30], and to promote glucose uptake by activating a signaling pathway that involves the phosphorylation of the Rab GTPase-activating protein AS160 (alternative name: Tbc1d4) that ultimately leads to the translocation of GLUT4 to the plasma membrane (Fig. 3a, b, e, f)[54] (see Supplementary Fig. 12 for a summary of this signaling network).

Interestingly, a recent study showed that CNO treatment of murine brown preadipocytes expressing the GqD designer receptor suppressed lipogenesis[55]. In agreement with this finding, ligand-mediated activation of endogenously expressed, G_q-coupled endothelin ET_{1A} receptors also inhibited the differentiation of brown adipocytes[55]. Mechanistic studies showed that G_q activation inhibits the differentiation of brown adipocytes via stimulation of the RhoA/ROCK pathway[55]. These observations underline the key role of G_q signaling in regulating the activity/differentiation of both white and brown adipocytes.

In a previous study, Imamura et al.[39] reported that single-cell microinjection of a $G\alpha_{q/11}$ antibody into 3T3-L1 adipocytes markedly inhibited insulin-induced GLUT4 translocation, suggesting that efficient insulin-stimulated GLUT4 translocation in adipocytes requires G_q signaling. However, our data strongly suggest that agents that can activate G_q signaling can promote glucose uptake into adipocytes in an insulin-independent fashion. It should also be noted that Imamura et al.[39] only studied cultured cells and did not explore the effect of G_q signaling on lipolysis.

By using adipo-$G_{q/11}$ KO mice and FR900359 (FR; $G_{q/11}$ inhibitor; 1 μM) as experimental tools, we demonstrated that the ability of insulin to stimulate glucose uptake by adipocytes and inhibit lipolysis did not require the presence of adipocyte $G_{q/11}$ under our experimental conditions (Supplementary Fig. 9). However, this finding does not exclude the possibility that insulin signaling is regulated by the activity of $G_{q/11}$ (or vice versa) in other cell types or physiological responses. The seemingly discrepant findings between the study by Imamura et al.[39] and our data may be due to differences in experimental conditions including the use of different cell lines and alternative strategies to interfere with adipocyte $G_{q/11}$ signaling.

IP_1 assays indicated that $G_{q/11}$ signaling was enhanced in adipose tissue (eWAT) of fasted WT mice (Supplementary Fig. 11). Since adipo-$G_{q/11}$ KO mice showed elevated plasma FFA levels under fasting conditions (Fig. 6i, Supplementary Fig. 8c), the IP_1 data suggest that adipocyte $G_{q/11}$ signaling plays a role in regulating the magnitude of fasting-induced lipolysis. As discussed above, activation of adipocyte $G_{q/11}$ signaling led to improved glucose tolerance in several mouse models. Since all glucose tolerance tests were carried out with fasted mice, it is possible that enhanced adipocyte $G_{q/11}$ signaling contributes to the removal of glucose from the blood, consistent with the notion that this pathway plays a role in maintaining glucose homeostasis.

In summary, by using a combined molecular genetic/biochemical/pharmacologic approach we provide strong evidence that activation of adipocyte G_q signaling in vitro and in vivo promotes glucose uptake and exerts a strong antilipolytic effect in an AMPK-dependent fashion. In a proof-of-concept study, we also demonstrate that agonist simulation of a G_q-coupled receptor ($CysLT_2$ receptor) endogenously expressed by adipocytes can overcome the metabolic deficits caused by impaired insulin receptor signaling in adipocytes. Importantly, our data clearly indicate that endogenous adipocyte $G_{q/11}$ signaling plays a physiological role in maintaining proper glucose and lipid homeostasis. These findings should pave the way toward the development of GPCR-based therapies aimed at restoring impaired adipocyte function in T2D and related metabolic disorders.

Methods

Generation and maintenance of mutant mice. Mutant mice expressing a G_q-coupled DREADD (hM3Dq; short name: GqD)[18] selectively in adipocytes (adipo-GqD mice) were generated by crossing *adipoq-Cre* mice (The Jackson Laboratory, stock # 010803) with *LSL-hM3Dq* mice (alternative name: *CAG-LSL-hM3Dq* mice)[20]. Mice that carried one copy of the *LSL-hM3Dq* gene but did not harbor the *adipoq-Cre* transgene served as control animals. Adipocyte-specific $G\alpha_{q/11}$[−/−] mice (adipo-$G_{q/11}$ KO mice) were created by crossing *adipoq-Cre* mice with $G\alpha_q$-*flox/flox* $G\alpha_{11}$[−/−] mice[56]. The generation of *adipoq-CreER^{T2}-AMPK β1 flox/flox β2flox/flox* mice has been described[37]. We also crossed IR*flox/flox* mice (The Jackson Laboratory, stock # 006955) with adipo-GqD mice, resulting in *adipo-GqD IR*^{+/−} mice. In studies where *adipo-GqD IR*^{+/−} mice were used, LSL-GqD-IR[+/flox] mice that do not carry the *adipoq-Cre* transgene served as control animals. All mouse strains were maintained on a C57BL/6 background.

All experiments were performed with adult male littermates, unless stated otherwise. Mice were housed at room temperature (23 °C; humidity: 30–40%) and provided with standard chow (7022 NIH-07 diet, 15% kcal fat, energy density 3.1 kcal/g; Envigo Inc.). Animals had free access to water and food and were kept on a 12-hr light/dark cycle. To induce obesity, 6–8-week-old male mice were switched to a high fat diet (HFD) (F3282, 60% kcal fat, energy density 5.5 kcal/g; Bio-Serv). Mice were maintained on the HFD for at least 8 weeks before initiating metabolic studies. All animal experiments were carried out according to the U.S. National Institutes of Health Guidelines for Animal Research and were approved by the National Institute of Diabetes and Digestive and Kidney Diseases Institutional Animal Care and Use Committee.

Body composition. The lean and fat mass composition of mutant and control mice was measured using the 3-in-1 Echo MRI Composition Analyzer (Echo Medical System).

In vivo metabolic tests. Male mice consuming regular chow (RC) or HFD were subjected to a series of in vivo metabolic tests. Adipo-GqD mice and control littermates that had been fasted for 4 hr received a single injection of CNO (10 mg/kg i.p.). Blood was collected from the tail vein just prior to injections (time '0') and at specific postinjection time points. Adipo-GqD-IR^{+/−} mutant mice and their corresponding control mice received CNO (10 mg/kg i.p.) or saline after a 4 h fast, followed by the collection of blood samples at specific time points. Blood glucose levels were measured using a portable glucometer (Contour Glucometer, Bayer). Plasma samples were obtained by centrifuging blood samples at 4 °C for 10 min at ~12,000x g. Plasma insulin levels were measured using an ELISA kit (Crystal Chem Inc.), according to the manufacturer's instructions. Plasma glycerol and FFA levels were determined using commercially available kits (Sigma-Aldrich). Plasma leptin levels were measured via ELISA (kit from R&D Systems).

For GTT studies, mice were fasted overnight for 16 h (unless stated otherwise) and then injected i.p. with a glucose bolus (RC mice: 2 g/kg; HFD mice: 1 g/kg) in the presence or absence of CNO (10 mg/kg i.p.). Blood glucose levels were determined at 0, 15, 30, 60, 90, and 120 min. For ITT studies, mice were fasted for 4 h and then injected i.p. with human insulin (0.75 or 1 U/kg: Humulin, Eli Lilly) in the absence or presence of CNO (10 mg/kg i.p.). Blood glucose levels were monitored at time '0' and at defined post-injection time points. To study GSIS, adipo-GqD and control mice were fasted 4 h and then injected i.p. with glucose (1 or 2 g/kg) in the absence or presence of CNO (10 mg/kg i.p.). Plasma insulin levels were measured at defined post-injection time points via ELISA.

Western blotting studies. Adipocytes/adipose tissues were lysed, and proteins were extracted using radioimmunoprecipitation assay (RIPA) buffer supplemented with cOmplete EDTA-free protease inhibitor cocktail (Sigma-Aldrich). Cell lysates were centrifuged at 12,000x g for 10 min, and protein concentrations were determined using a BCA protein assay kit (Pierce). Subsequently, proteins samples were denatured at 95 °C using NuPAGE LDS sample buffer (Thermo Fisher Scientific), and proteins were separated via 4–12% SDS–polyacrylamide gel electrophoresis. Proteins were then transferred to nitrocellulose membranes and incubated overnight at 4 °C with primary antibody. On the next day, membranes were washed thoroughly and then incubated with HRP-conjugated anti-rabbit or anti-goat secondary antibody, followed by visualization of separated protein bands using SuperSignal West Pico Chemiluminescent Substrate (Thermo Fisher Scientific) on the c600 Imaging System Imager (Azure Biosystems). Immunoreactive bands were quantified using Image J Software (NIH). Uncropped images are provided in the Source Data file.

The following antibodies were used (source, catalog #, if applicable, and dilution are indicated): AMPKα (Cell Signaling Technology, #2532, 1:1000), AMPKβ 1/2 (Dr. Gregory Steinberg, 1:1000), phospho-AMPKα (Thr172) (40H9) (Cell Signaling Technology, #2535, 1:1000), AS160 (Abcam, #134749, 1:2,000), phospho-AS160 (Thr642) (D27E6) (Cell Signaling Technology, #8881, 1:1000), HSL (Cell Signaling Technology, #4107, 1:1000), phospho-HSL (Ser565) (Cell Signaling Technology, #4137, 1:1,000), Glut4 (1F8) (Cell Signaling Technology, #2213, 1:1000), Na,K-ATPase (Cell Signaling Technology, #3010, 1:1000), HA-tag (C29F4) (Cell Signaling Technology, #3724, 1:1000), β-actin (13E5) (Cell Signaling Technology, #4970, 1:1000), anti-mouse IgG, HRP-linked antibody (Cell Signaling Technology #7076, 1:2000), antirabbit IgG, HRP-linked antibody (Cell Signaling Technology #7074, 1:2000).

qRT-PCR analysis of gene expression. Total RNA was extracted from frozen tissues or cultured cells using the RNeasy mini kit (Qiagen), and SuperScript III First-Strand Synthesis SuperMix (Invitrogen) was used to prepare cDNA. The SYBR green method (Applied Biosystems) was used to perform quantitative PCR studies[57]. Gene expression data were normalized relative to the expression of 18 S rRNA using the ΔΔCt method. All PCR primers used in this study are listed in Supplementary Table 3.

Differentiation of 3T3F442A cells. Mouse 3T3F442A cells (Kerafast, catalog # EF3002) were incubated with Dulbecco's minimum essential medium (DMEM) containing 10% bovine calf serum (BCS) and 1% pen/strep in a 10% CO_2 incubator at 37 °C. Cells were grown in 12-well collagen-coated plates. Once the cells had reached confluence, they were differentiated into mature adipocytes by a two-day incubation with DMEM containing 10% BCS, insulin (0.5 µg/ml), IBMX (250 µM), dexamethasone (0.5 µM), indomethacin (60 µM), and rosiglitazone (2 µM). After this treatment, cells were grown in DMEM containing 10% BCS and insulin (0.5 µM) for 48 hr. Subsequently, cells were maintained in DMEM containing 10% BCS and used for experiments.

siRNA-mediated knockdown of AS160 and HSL expression in 3T3F442A cells. AS160 siRNA (mouse *Tbc1d4* siRNA) was purchased from Santa Cruz. HSL siRNA (*Lipe* smart pool mouse siRNA) and scrambled control siRNA were obtained from Dharmacon. On day 0, 3T3F442A cells were transfected with siRNA using Lipofectamine RNAiMAX (Thermo Fisher Scientific) by following the manufacturer's instructions. Four hr later, cells were changed to differentiation media. On day 5, differentiated 3T3F442A adipocytes were used for further experiments.

Isolation and differentiation of mouse preadipocytes. Mouse preadipocytes were isolated and differentiated using a standard protocol[40]. In brief, inguinal WAT (iWAT) was isolated from 8–10-week-old male mice and digested using collagenase 1 (Sigma–Aldrich) in Krebs-Ringer Hepes bicarbonate buffer (KRH buffer: 120 mM NaCl, 4 mM KH_2PO_4, 1 mM $MgSO_4$, 1 mM $CaCl_2$, 10 mM $NaHCO_3$, and 30 mM HEPES; pH = 7.4). Digested tissue was passed through a 10 µm cell strainer and centrifuged at 300x g for 5 min at room temperature. The resulting cell pellet was resuspended and then filtered through a 40 µm cell strainer, and the resultant cell suspension was centrifuged (same conditions as above). Finally, the cell pellet was resuspended in DMEM containing 10% fetal bovine serum (FBS), supplemented with 1% pen/strep. Cells were grown in 12-well collagen-coated plates. Once the preadipocytes reached 100% confluency, they were differentiated into mature adipocytes by a two-day incubation with differentiation media containing insulin, IBMX, rosiglitazone, dexamethasone, and indomethacin (for details, see the previous paragraph). After this period, cells were incubated with DMEM containing 10% FBS, 0.5 µM insulin, and, when required, 100 nM 4-hydroxytamoxifen[37] for another 48 h. Differentiated mouse adipocytes were then used for functional experiments.

Preparation of differentiated human white adipocytes. Immortalized human white preadipocytes (hWAT-SVF cells; kindly provided by Dr. Yu-Hua Tseng, Joslin Diabetes Center, Boston, MA)[34] were plated in collagen-coated 6- or 12-well plates and maintained in DMEM supplemented with 10% FBS and 1% pen/strep in a 5% CO_2 incubator at 37 °C. Once cells reached 100% confluency, they were treated with induction media containing human insulin (0.5 µM), biotin (33 µM), pantothenate (17 µM), dexamethasone (0.1 µM), IBMX (500 µM), indomethacin (30 µM), and T3 (2 nM) for 28 days. Once the differentiation process was complete, media were replaced with DMEM containing 10% FBS.

Adenoviruses. The adenovirus coding for hM3Dq (short name: GqD) (titer: 1.2 × 10^{12} transducing units/ml) was generated by the University of North Carolina at Chapel Hill Vector Core (Director: Dr. David Dismuke). The hM3Dq coding sequence[18] was inserted into the pShuttle-CMV-IRES-mCitrine vector. The adenovirus coding for GFP (titer: 3.2 × 10^{11} IFU/mL) was a gift from the laboratory of Dr. Marc Montminy (Salk Institute for Biological Studies, La Jolla, CA). Adenoviruses were added to the growth medium at a multiplicity of infection of 50 MOI one day before the end of the adipocyte differentiation step (4 days after the start of differentiation). On the following day, the medium was replaced with fresh one. Assays were performed two days after the addition of viruses.

In vivo tissue glucose uptake assay. Adipo-GqD mice and control littermates maintained on regular chow were subjected to in vivo tissue glucose uptake studies. In brief, mice were fasted overnight for 16 h and then injected i.p. with either saline or CNO (10 mg/kg) containing a trace amount of ^{14}C-2-deoxyglucose (10 µCi; PerkinElmer). Forty minutes after injection, mice were euthanized, and multiple metabolically active tissues were collected, weighed, and homogenized. Radioactivity was measured as described[58].

Adipocyte glucose uptake assay. In vitro glucose uptake by adipocytes was determined following a published protocol[14]. Cells were grown in 12-well collagen-coated plates. On the day of experiment, differentiated adipocytes prepared from 3T3F442A cells or mouse pre-adipocytes were serum-starved for 3 hr and then washed with HBS buffer of the following composition (in mM): 20 HEPES [pH 7.4], 2.5 $MgSO_4$, 1 $CaCl_2$, 140 NaCl, and 5 KCl. Adipocytes were then incubated with various pharmacological agents as described in the text. Subsequently, cells were incubated with HBS buffer containing 0.5 µCi/ml ^{3}H-2-deoxy-glucose (PerkinElmer) and 100 µM 2-deoxy-D-glucose (Sigma). Nonspecific glucose uptake was measured in the presence of 10 µM cytochalasin B (Sigma-Aldrich). Finally, stop solution (0.9% NaCl solution containing 25 mM glucose) was added to terminate glucose uptake. Adipocytes were then lysed with 0.05 N NaOH, and radioactivity was measured with a PerkinElmer liquid scintillation counter. Protein concentrations were determined by using the Bio-Rad Bradford assay kit. Glucose uptake was calculated as uptake of ^{3}H-2-deoxy-glucose (in pmoles) per mg of protein (pmoles/mg/min).

In vitro lipolysis assay. Differentiated 3T3F442A cells, hWAT cells, and mouse primary adipocytes were used for lipolysis measurements. Cells were grown in 12-well collagen-coated plates. Cells were serum-starved with DMEM basal media for 2 h, and then incubated with various pharmacological agents dissolved in DMEM for 3 h at 37 °C, as indicated in the text. Subsequently, the amount of glycerol released into the medium was determined as a measure of lipolysis. Cells were lysed using RIPA buffer to measure protein concentrations. Lipolysis data were expressed as the amount of glycerol released per mg of cellular protein. In the case of hWAT cells, KRB buffer (composition in mM: 135 NaCl, 5 KCl, 1 $MgSO_4$, 0.4 K_2HPO_4, 20 HEPES, 1 $CaCl_2$, 5 glucose, and 4% BSA; pH=7.4) served as assay buffer.

GLUT4 translocation measured with differentiated 3T3-F442A cells. 3T3-F442A cells were grown in 6-well collagen-coated plates. The cells were infected with GqD- or GFP-encoding adenoviruses (50 MOI) one day before the end of the differentiation step (4 days after the start of differentiation). After the addition of new media, the cells were incubated for 48 h with a GLUT4-myc-expressing adenovirus (50 MOI) (a kind gift by Dr. Susanna Keller, University of Virginia, Charlottesville, VA) 5 days after the start of the differentiation step. Subsequently, cells were incubated with CNO (10 μM) for 30 min, and plasma membranes were prepared as described using a standard protocol[59]. In brief, cells were homogenized in a buffer containing 250 mM sucrose, 10 mM Tris HCl, and 1 mM EDTA. Homogenates were centrifuged at 960 x g for 2 min at 4 °C. The resultant supernatant was centrifuged at 20,000 x g for 20 min at 4 °C. The pellet was resuspended in buffer and centrifuged at 160,000 x g for 60 min. Subsequently, the pellet was resuspended and re-centrifuged at 150,000 x g for 60 min. The amount of GLUT4 present in the resulting plasma membrane pellet was quantitated via western blotting using a commercially available mouse monoclonal anti-GLUT4 antibody (Cell Signaling Technology, #2213).

CAMKK2 assay. Differentiated 3T3F442A cells infected with the GqD adenovirus (GqD-3T3F442A cells) were used to measure CAMKK2 activity. Cells were grown in 12-well collagen-coated plates. On the day of the experiment, GqD-3T3F442A cells were serum starved for 3 h and then treated with CNO (10 μM) or CNO (10 μM) plus STO-609 (20 μM) for 30 min. Subsequently, the cells were lysed, and CAMKK2 activity was measured using the CycLex® CaMKKβ Kinase Assay Kit (MBL International Corporation), following the manufacturer's instructions.

Treatment of mice with a selective CysLT$_2$ receptor agonist. Adipo-GqD-IR $^{+/-}$ mutant mice and control littermates lacking the *adipoq-Cre* transgene that had been maintained on HFD for 12 weeks were injected with N-methyl LTC$_4$ (NMLTC$_4$; 10 μg/kg i.p.), a hydrolysis-resistant, selective CysLT$_2$ receptor agonist[41], followed by the measurement of blood glucose and plasma FFA levels. In glucose tolerance testes, MLTC$_4$ (10 μg/kg) was co-injected i.p. with 1 g/kg of glucose.

Ex vivo IP$_1$ assay with mouse adipose tissues. Twelve male WT C57BL/6 mice (age: 8 weeks; Taconic) were injected with LiCl (10 mmoles/kg, s.c.) prior to the beginning of the dark cycle (6 pm). Six mice had free access to food, while the remaining six mice were fasted overnight. On the next morning (8 am), the mice were euthanized, and adipose depots (iWAT and eWAT) were isolated and quickly frozen on dry ice. Adipose tissues were homogenized in RIPA buffer, supplemented with LiCl (50 mM) and complete EDTA-free protease inhibitor cocktail (Roche). Briefly, 100–200 mg tissue was incubated in RIPA buffer with LiCl (50 mM) for 15 min on ice, followed by homogenization in lysing matrix E tubes using a Precellys® 24 homogenizer. The resultant supernatant was subjected to centrifugation (6000 x g) for 15 min to separate the 'fat cake' (white lipid layer) from the supernatant containing the loose pellet. The supernatant and the loose pellet (cell debris) were subjected to an additional centrifugation step (1200 x g, 15 min) to yield the protein lysate (supernatant). IP$_1$ levels in the protein lysates were measured using the IP-one ELISA kit from Cisbio following the manufacturer's instructions.

Source of human subcutaneous adipose tissue. We complied with all relevant ethical regulations for work with human participants. Subjects were admitted to the Metabolic Clinical Research Unit in the Hatfield Clinical Research Center of the National Institutes of Health (Bethesda, MD) to participate in an NIDDK/NIAMS institutional review board-approved protocol (ClinicalTrials.gov identifier NCT00428987), after having given informed consent. The human adipose tissue samples analyzed in this study have been described in detail in a recent study[40]. Human subcutaneous fat tissue samples were obtained from the abdominal area under local anesthesia using an aspiration needle. After the isolation of mRNA, gene expression levels were determined via qRT-PCR.

Statistics. Data were collected and analyzed by using Prism 8 (GraphPad) and Microsoft Excel software. All data are expressed as means ± s.e.m. for the indicated number of observations. Prior to performing specific statistical tests, we performed tests for normality and homogeneity of variance. Data were then tested for statistical significance by one- or two-way ANOVA, followed by the indicated post hoc tests, or by using a two-tailed unpaired Student's t test, as appropriate. Correlation analysis was conducted by Spearman's test. A p value of <0.05 was considered statistically significant. The specific statistical tests that were used are indicated in the figure legends.

Reporting summary. Further information on research design is available in the Nature Research Reporting Summary linked to this article.

Data availability

All data generated or analyzed during this study are included in this published article (and its supplementary information files). Source data are provided as a Source Data file. Source data are provided with this paper.

References

1. Guilherme, A., Virbasius, J. V., Puri, V. & Czech, M. P. Adipocyte dysfunctions linking obesity to insulin resistance and type 2 diabetes. *Nat. Rev. Mol. Cell Biol.* **9**, 367–377 (2008).
2. Kusminski, C. M., Bickel, P. E. & Scherer, P. E. Targeting adipose tissue in the treatment of obesity-associated diabetes. *Nat. Rev. Drug Disco.* **15**, 639–660 (2016).
3. Scherer, P. E. The many secret lives of adipocytes: implications for diabetes. *Diabetologia* **62**, 223–232 (2019).
4. Duncan, R. E., Ahmadian, M., Jaworski, K., Sarkadi-Nagy, E. & Sul, H. S. Regulation of lipolysis in adipocytes. *Annu. Rev. Nutr.* **27**, 79–101 (2007).
5. DeFronzo, R. A. et al. Type 2 diabetes mellitus. *Nat. Rev. Dis. Prim.* **1**, 15019 (2015).
6. Wang, L. et al. Use of DREADD Technology to Identify Novel Targets for Antidiabetic Drugs. *Annu Rev. Pharm. Toxicol.* **61**, 421–440 (2021).
7. Riddy, D. M., Delerive, P., Summers, R. J., Sexton, P. M. & Langmead, C. J. G Protein-Coupled Receptors Targeting Insulin Resistance, Obesity, and Type 2 Diabetes Mellitus. *Pharm. Rev.* **70**, 39–67 (2018).
8. Ahren, B. Islet G protein-coupled receptors as potential targets for treatment of type 2 diabetes. *Nat. Rev. Drug Disco.* **8**, 369–385 (2009).
9. Sriram, K. & Insel, P. A. G Protein-Coupled Receptors as Targets for Approved Drugs: How Many Targets and How Many Drugs? *Mol. Pharm.* **93**, 251–258 (2018).
10. Pierce, K. L., Premont, R. T. & Lefkowitz, R. J. Seven-transmembrane receptors. *Nat. Rev. Mol. Cell Biol.* **3**, 639–650 (2002).
11. Amisten, S. et al. An atlas of G-protein coupled receptor expression and function in human subcutaneous adipose tissue. *Pharm. Ther.* **146**, 61–93 (2015).
12. Regard, J. B., Sato, I. T. & Coughlin, S. R. Anatomical profiling of G protein-coupled receptor expression. *Cell* **135**, 561–571 (2008).
13. Wettschureck, N. & Offermanns, S. Mammalian G proteins and their cell type specific functions. *Physiological Rev.* **85**, 1159–1204 (2005).
14. Wang, L. et al. Adipocyte G(i) signaling is essential for maintaining whole-body glucose homeostasis and insulin sensitivity. *Nat. Commun.* **11**, 2995 (2020).
15. Wang, L. et al. Selective activation of Gs signaling in adipocytes causes striking metabolic improvements in mice. *Mol. Metab.* **27**, 83–91 (2019).
16. Caron, A. et al. Adipocyte Gs but not Gi signaling regulates whole-body glucose homeostasis. *Mol. Metab.* **27**, 11–21 (2019).
17. Chaves, V. E., Frasson, D. & Kawashita, N. H. Several agents and pathways regulate lipolysis in adipocytes. *Biochimie* **93**, 1631–1640 (2011).
18. Armbruster, B. N., Li, X., Pausch, M. H., Herlitze, S. & Roth, B. L. Evolving the lock to fit the key to create a family of G protein-coupled receptors potently activated by an inert ligand. *Proc. Natl Acad. Sci. USA* **104**, 5163–5168 (2007).
19. Rogan, S. C. & Roth, B. L. Remote control of neuronal signaling. *Pharm. Rev.* **63**, 291–315 (2011).
20. Zhu, H. et al. Cre-dependent DREADD (Designer Receptors Exclusively Activated by Designer Drugs) mice. *Genes. (N. Y., N. Y.: 2000)* **54**, 439–446 (2016).
21. Eguchi, J. et al. Transcriptional control of adipose lipid handling by IRF4. *Cell Metab.* **13**, 249–259 (2011).
22. Nagai, Y. et al. Deschloroclozapine, a potent and selective chemogenetic actuator enables rapid neuronal and behavioral modulations in mice and monkeys. *Nat. Neurosci.* **23**, 1157–1167 (2020).
23. Camporez, J. P. et al. Anti-inflammatory effects of oestrogen mediate the sexual dimorphic response to lipid-induced insulin resistance. *J. Physiol.* **597**, 3885–3903 (2019).
24. Pettersson, U. S., Waldén, T. B., Carlsson, P. O., Jansson, L. & Phillipson, M. Female mice are protected against high-fat diet induced metabolic syndrome and increase the regulatory T cell population in adipose tissue. *PLoS One* **7**, e46057 (2012).
25. Taegtmeyer, H. Energy metabolism of the heart: from basic concepts to clinical applications. *Curr. Probl. Cardiol.* **19**, 59–113 (1994).
26. Depre, C., Vanoverschelde, J. L. & Taegtmeyer, H. Glucose for the heart. *Circulation* **99**, 578–588 (1999).
27. Schrage, R. et al. The experimental power of FR900359 to study Gq-regulated biological processes. *Nat. Commun.* **6**, 10156 (2015).
28. Yamaguchi, S. et al. Activators of AMP-activated protein kinase enhance GLUT4 translocation and its glucose transport activity in 3T3-L1 adipocytes. *Am. J. Physiol. Endocrinol. Metab.* **289**, E643–E649 (2005).
29. Haemmerle, G., Zimmermann, R. & Zechner, R. Letting lipids go: hormone-sensitive lipase. *Curr. Opin. Lipido.* **14**, 289–297 (2003).

30. Nielsen, T. S., Jessen, N., Jørgensen, J. O., Møller, N. & Lund, S. Dissecting adipose tissue lipolysis: molecular regulation and implications for metabolic disease. *J. Mol. Endocrinol.* **52**, R199–R222 (2014).

31. Watt, M. J. & Steinberg, G. R. Regulation and function of triacylglycerol lipases in cellular metabolism. *Biochem J.* **414**, 313–325 (2008).

32. Marcelo, K. L., Means, A. R. & York, B. The Ca(2+)/Calmodulin/CaMKK2 Axis: Nature's Metabolic CaMshaft. *Trends Endocrinol. Metab.: TEM* **27**, 706–718 (2016).

33. Robidoux, J., Martin, T. L. & Collins, S. Beta-adrenergic receptors and regulation of energy expenditure: a family affair. *Annu Rev. Pharm. Toxicol.* **44**, 297–323 (2004).

34. Xue, R. et al. Clonal analyses and gene profiling identify genetic biomarkers of the thermogenic potential of human brown and white preadipocytes. *Nat. Med.* **21**, 760–768 (2015).

35. Collins, S. & Surwit, R. S. The beta-adrenergic receptors and the control of adipose tissue metabolism and thermogenesis. *Recent Prog. Horm. Res.* **56**, 309–328 (2001).

36. Revelli, J. P., Muzzin, P., Paoloni, A., Moinat, M. & Giacobino, J. P. Expression of the beta 3-adrenergic receptor in human white adipose tissue. *J. Mol. Endocrinol.* **10**, 193–197 (1993).

37. Mottillo, E. P. et al. Lack of adipocyte AMPK exacerbates insulin resistance and hepatic steatosis through brown and beige adipose tissue function. *Cell Metab.* **24**, 118–129 (2016).

38. Wettschureck, N. et al. Absence of pressure overload induced myocardial hypertrophy after conditional inactivation of Galphaq/Galpha11 in cardiomyocytes. *Nat. Med.* **7**, 1236–1240 (2001).

39. Imamura, T. et al. G alpha-q/11 protein plays a key role in insulin-induced glucose transport in 3T3-L1 adipocytes. *Mol. Cell. Biol.* **19**, 6765–6774 (1999).

40. Pydi, S. P. et al. Adipocyte beta-arrestin-2 is essential for maintaining whole body glucose and energy homeostasis. *Nat. Commun.* **10**, 2936 (2019).

41. Yan, D. et al. Differential signaling of cysteinyl leukotrienes and a novel cysteinyl leukotriene receptor 2 (CysLT$_2$) agonist, N-methyl-leukotriene C$_4$, in calcium reporter and β arrestin assays. *Mol. Pharm.* **79**, 270–278 (2011).

42. Wunder, F. et al. Pharmacological characterization of the first potent and selective antagonist at the cysteinyl leukotriene 2 (CysLT(2)) receptor. *Br. J. Pharmacol.* **160**, 399–409 (2010).

43. Gastaldelli, A., Gaggini, M. & DeFronzo, R. A. Role of adipose tissue insulin resistance in the natural history of Type 2 Diabetes: Results from the San Antonio Metabolism Study. *Diabetes* **66**, 815–822 (2017).

44. Qiang, G. et al. Lipodystrophy and severe metabolic dysfunction in mice with adipose tissue-specific insulin receptor ablation. *Mol. Metab.* **5**, 480–490 (2016).

45. Trinquet, E., Bouhelal, R. & Dietz, M. Monitoring Gq-coupled receptor response through inositol phosphate quantification with the IP-One assay. *Expert Opin. Drug Disco.* **6**, 981–994 (2011).

46. Moore, A. R. et al. Recurrent activating mutations of G-protein-coupled receptor CYSLTR2 in uveal melanoma. *Nat. Genet* **48**, 675–680 (2016).

47. Lawrence, J. T. & Birnbaum, M. J. ADP-ribosylation factor 6 delineates separate pathways used by endothelin 1 and insulin for stimulating glucose uptake in 3T3-L1 adipocytes. *Mol. Cell. Biol.* **21**, 5276–5285 (2001).

48. Kishi, K. et al. Gq-coupled receptors transmit the signal for GLUT4 translocation via an insulin-independent pathway. *J. Biol. Chem.* **271**, 26561–26568 (1996).

49. Ali, S. B., Turner, J. J. O. & Fountain, S. J. Constitutive P2Y(2) receptor activity regulates basal lipolysis in human adipocytes. *J. Cell Sci.* **131**, jcs221994 (2018).

50. Yue, P. et al. Apelin decreases lipolysis via G(q), G(i), and AMPK-dependent mechanisms. *Endocrinology* **152**, 59–68 (2011).

51. Kishi, K. et al. AMP-Activated protein kinase is activated by the stimulations of G(q)-coupled receptors. *Biochemical biophysical Res. Commun.* **276**, 16–22 (2000).

52. Hutchinson, D. S. & Bengtsson, T. AMP-activated protein kinase activation by adrenoceptors in L6 skeletal muscle cells: mediation by alpha1-adrenoceptors causing glucose uptake. *Diabetes* **55**, 682–690 (2006).

53. Kahn, B. B., Alquier, T., Carling, D. & Hardie, D. G. AMP-activated protein kinase: ancient energy gauge provides clues to modern understanding of metabolism. *Cell Metab.* **1**, 15–25 (2005).

54. Sakamoto, K. & Holman, G. D. Emerging role for AS160/TBC1D4 and TBC1D1 in the regulation of GLUT4 traffic. *Am. J. Physiol. Endocrinol. Metab.* **295**, E29–E37 (2008).

55. Klepac, K. et al. The Gq signalling pathway inhibits brown and beige adipose tissue. *Nat. Commun.* **7**, 10895 (2016).

56. Sassmann, A. et al. The Gq/G11-mediated signaling pathway is critical for autocrine potentiation of insulin secretion in mice. *J. Clin. Invest* **120**, 2184–2193 (2010).

57. Jain, S. et al. Chronic activation of a designer G(q)-coupled receptor improves beta cell function. *J. Clin. Invest* **123**, 1750–1762 (2013).

58. Kim, J. K., Gavrilova, O., Chen, Y., Reitman, M. L. & Shulman, G. I. Mechanism of insulin resistance in A-ZIP/F-1 fatless mice. *J. Biol. Chem.* **275**, 8456–8460 (2000).

59. Bone, D. B. J. et al. Skeletal muscle-specific activation of Gq Signaling maintains glucose homeostasis. *Diabetes* **68**, 1341–1352 (2019).

Author contributions

T.K., S.P.P., and J.W. designed the study and researched data. T.K., S.P.P., L.W., D.H., Y.C., H.L., and O.G. carried out experiments and interpreted and analyzed experimental data. E.K., G.M.K., and G.R.S. provided key reagents/mouse strains and helpful advice. T.K. and J.W. wrote the manuscript.

Competing interests

The authors declare no competing interests.

Additional information

Supplementary information The online version contains supplementary material available at https://doi.org/10.1038/s41467-022-29231-6.

Correspondence and requests for materials should be addressed to Jürgen Wess.

Peer review information *Nature Communications* thanks the other anonymous reviewer(s) for their contribution to the peer review of this work.

Reprints and permission information is available at http://www.nature.com/reprints

Publisher's note Springer Nature remains neutral with regard to jurisdictional claims in published maps and institutional affiliations.